TELIC-80-1

DEVELOPMENT OF SELECTIVE SURFACES

Final Technical Progress Report for Period September 11, 1978—March 31, 1980

By
John A. Thornton
James L. Lamb
Alan S. Penfold

August 15, 1980

Work Performed Under Contract No. AC04-78CS35306

Telic Corporation
Santa Monica, California

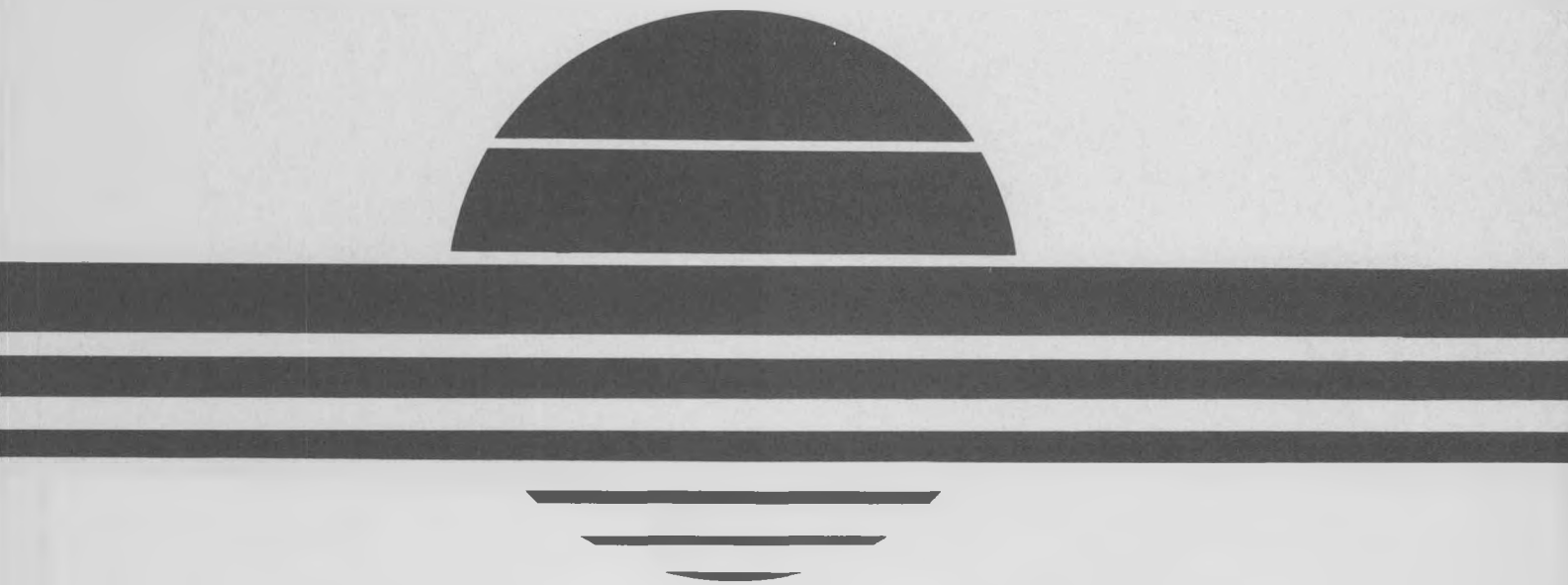

U.S. Department of Energy

Solar Energy

TELIC-80-1
Distribution Category UC-59c

DEVELOPMENT OF SELECTIVE SURFACES

Final Technical Progress Report

Period: September 11, 1978 - March 31, 1980

By

John A. Thornton, James L. Lamb, and Alan S. Penfold

Telic Corporation
1631 Colorado Avenue
Santa Monica, California 90404

August 15, 1980

Work Performed Under Contract No. DE-AC04-78CS35306

Department of Energy
Albuquerque Operations Office
P.O. Box 5400
Albuquerque, New Mexico 87115

TABLE OF CONTENTS

LIST OF TABLES AND FIGURES

Page

ABSTRACT

This is the final report covering work conducted at Telic Corporation over the period September 11, 1978, to March 31, 1980, on Department of Energy Contract DE-AC04-78CS35306.

Recent advances in sputtering technology using magnetically confined plasmas in so-called "magnetron configurations" permit coatings to be deposited over large areas with significantly increased deposition rates. Work is described in which cylindrical-post magnetron sources were used to deposit cermet type selective absorber coatings by reactively sputtering both stainless steel and chromium in Ar-O_2 and in Ar-CO gas mixtures. In addition, Cr/Al_2O_3 graded cermet coatings were deposited by co-sputtering from Cr and Al_2O_3 post-magnetron sources. The substrates were aluminum foil and aluminum-coated glass. In other work, multi-layer Al_2O_3-Mo-Al_2O_3 coatings were deposited using both cylindrical-post and hollow magnetron sources. Both reactive sputtering and direct rf sputtering of alumina were used to form the Al_2O_3 layers. The substrates were molybdenum-coated stainless steel and glass.

All of the coatings yielded hemispherical absorptances (α_H) of 0.90 or more and hemispherical emittances (ϵ_H) at 20°C of 0.10 or less. However, the Al_2O_3-Mo-Al_2O_3 coatings yielded the best optical performance (α_H = 0.95, ϵ_H = 0.06) and thermal stability (550°C in air and 700°C in vacuum).

1. PROJECT DESCRIPTION

Recent advances in sputtering technology using magnetically confined plasmas permit coatings to be deposited over large areas with significantly increased deposition rates.[1] The objective of this project was to develop methods for producing low cost selective absorber surfaces using one form of magnetically enhanced sputtering source: the cylindrical magnetron.[2,3]

In a four-phase program, two representative selective absorber coatings, with wide potential for application, were investigated as vehicles for evaluating the sputtering technology. In one phase a sputter-deposited form of the graded $Cr\text{-}Cr_2O_3$ cermet coating that is formed by electroplating (black chrome) was examined to illustrate the capabilities of sputtering for forming cermet type coatings. In a second phase a sputter-deposited form of the $Al_2O_3\text{-}Mo\text{-}Al_2O_3$ (AMA) coating that has been found to have excellent thermal stability was examined to illustrate the multi-layer capabilities of sputtering.

Particular attention was given during the cermet work to the deposition of coatings onto aluminum foil for subsequent attachment to flat plate collectors. In one proof-of-concept phase sputtered cermet type coatings were continuously deposited by reactive sputtering onto aluminum foil strip. In a second proof of concept phase $Al_2O_3\text{-}Mo\text{-}Al_2O_3$ coatings were deposited onto short tubular sections using cylindrical-hollow magnetrons.

The optical properties of the coatings were evaluated at the Lockheed Palo Alto Research Laboratory. Hemispherical reflectance measurements were made over the wavelength range from 400 to 1800 nm. Air mass-two absorptances were calculated from these measurements. Room temperature total hemispherical emittance measurements were made using a Gier Dunkle infrared reflectometer. Thus, unless otherwise noted, the optical properties quoted in this report were measured at Lockheed.

The project was begun on 11 September 1978 and was scheduled for completion on 11 December 1979. Progress during the first few months was delayed

by the late delivery of equipment. Therefore the project was extended at no additional cost to 31 March 1980.

The basic principles of magnetron and reactive sputtering were reviewed in the Semi-Annual Technical Progress Report.[4] The reactive sputtering methods used to deposit the Phase I cermet coatings and the properties of these coatings were also described in detail in that report. Therefore, the Phase I results are simply summarized in this report. The emphasis here is on the Phase II Al_2O_3-Mo-Al_2O_3 work. The Phase III and Phase IV proof of concept experiments are also described.

2. WORK STATEMENT

The project was divided into four phases as described above. The specific tasks are listed below.

Phase I - Cermet Coatings

Task 1 - Investigate the selective absorber properties of thin coatings of chromium oxide and stainless steel oxide deposited by reactive sputtering onto aluminum foil substrates using cylindrical magnetron sputtering sources.

Task 2 - Investigate the selective absorber properties of multilayer coatings consisting of alternate diffuse layers of metal (chromium or stainless steel) and metal oxide deposited by reactive sputtering onto aluminum foil substrates using cylindrical magnetron sputtering sources.

Task 3 - Investigate the selective absorber properties of mixed metal/metal-oxide coatings (chromium or stainless steel) deposited by dual-source cylindrical magnetron sputtering onto aluminum foil substrates.

Phase II - Al_2O_3-Mo-Al_2O_3

Investigate the influence of deposition conditions and coating thickness on the selective absorption properties of Al_2O_3-Mo-Al_2O_3 coatings deposited on flat stainless steel substrates using dual-cathode cylindrical magnetron sputtering source.

Phase III - Cermet Proof-of-Concept

Conduct proof-of-concept experiments in which metal/metal-oxide

selective absorber coatings are deposited onto a continuous strip of aluminum foil using pay-off and take-up reels located within a vacuum chamber.

Phase IV - Al_2O_3-Mo-Al_2O_3 Proof-of-Concept

Conduct proof-of-concept experiments in which Al_2O_3-Mo-Al_2O_3 coatings are deposited onto the outside diameter of tubular stainless steel substrates by direct or reactive sputtering using hollow cathode magnetron sputtering sources.

3. PHASE I - CERMET COATINGS

3.1 Background Considerations

An effective selective surface can be formed by overcoating a low emittance surface with a material having a minimum reflectance at its top surface (low index of refraction), a high solar absorptance (high extinction coefficient), and a high infrared transparency. Single coating materials with the required combination of properties are not available.[5] However, the desired result can be obtained by placing a partially absorbing layer between the substrate and a nonabsorbing antireflective-type surface layer as shown in Fig. 1.[6] A cermet may be used as the partially absorbing layer. A cermet with graded metal content is a special case of the coating shown in Fig. 1. Scanning electron microscopy, Auger spectroscopy, and electron and X-ray diffraction studies of electroplated black chrome deposits indicate that they are essentially graded cermet type coatings consisting of Cr particle in a chromium oxide matrix or with chromium oxide surface layers.[7-9]

The objective of the Phase I investigation was to examine selective absorber coatings consisting of sputter-deposited chromium/chromium-oxide and stainless steel/stainless steel oxide cermet layers.

3.2 Single Layer Oxide Coatings (Task 1)

The primary objective of this task was to provide reference data for use in the other work. Chromium oxide and stainless steel oxide coatings

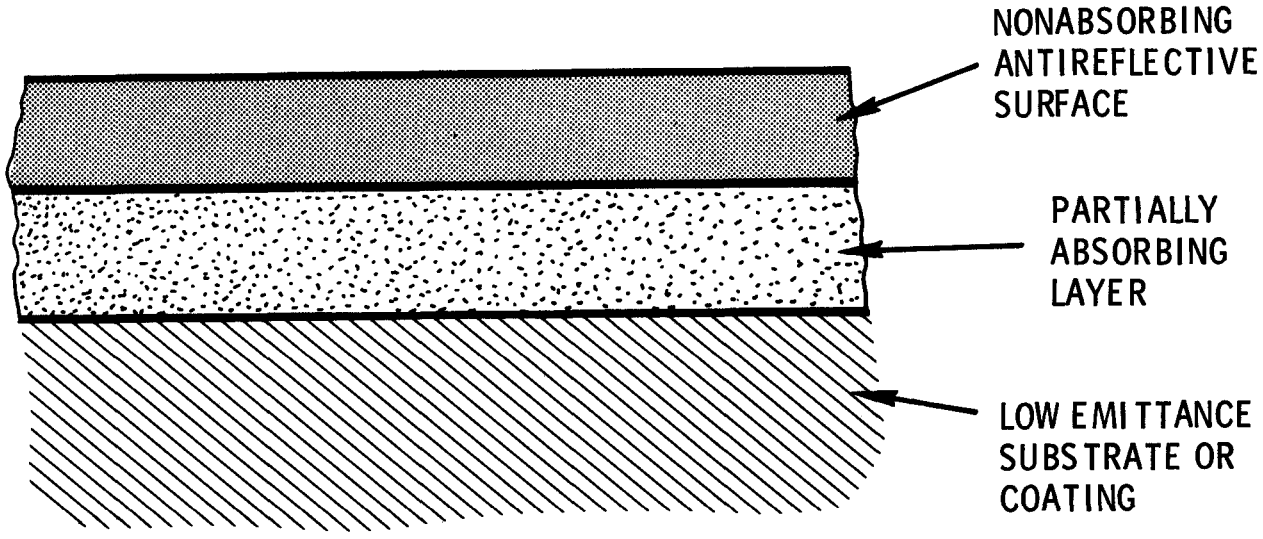

FIG. 1. Selective absorber coating configuration

were formed by reactive sputtering from chromium and stainless steel (type 304) cylindrical magnetron targets using pure oxygen in the pressure range 0.13 to 4 Pa (1 to 30 mTorr) as a working gas.[4] Cathode current densities, voltages, and deposition rates were 8 mA/cm^2, 650V and 0.3 nms for the chromium oxide and 8 mA/cm^2, 500V and 0.15 nm/s for the stainless steel oxide.

X-ray diffraction measurements* on both the chromium oxide and stainless steel oxide coatings yielded amorphous type diffraction patterns, which, according to the Scherrer line broadening formula, imply maximum crystallite sizes of 6-10Å. For the stainless steel oxide case the broad amorphous signal is centered at a point close to the 2.70Å d-spacing for alpha Fe_2O_3. The results of an ESCA analysis are shown in Table I (see page 12). For the chromium oxide case the broad peak appears to correspond to a CrO_2 line.

The optical constants (n,k) were determined over the wavelength range from 350 nm to 700 nm from transmission and reflectance measurements (glass) substrates) using curves** generated by Hadley.[10] The refractive indexes

---

* The X-ray diffraction measurements were made at Technology of Materials, Santa Barbara, CA. The samples were 2000 nm thick films deposited onto glass substrates. The measurements were made by aligning the samples in the plane of diffraction of a Phillips Electronics diffractometer equipped with a crystal monochrometer. The X-rays were generated from a Cu target with a 40 kV accelerating voltage.

**The Hadley curves give calculated values of the reflectance r and the transmittance t as a function of d/λ (d is the coating thickness and λ is the wavelength) for various values of the index of refraction n and extinction coefficient k. The curves are arranged with each set corresponding to a given value of k. Thus n and k values for a given film are determined by finding the Hadley curve set (k-value) for which the measured r and t values correspond to identical values of n at the measured d/λ. This is done by plotting, at the known d/λ, the n versus k combinations which satify the measured r and the combination which satisfies the measured t. The cross-over point of the two curves is then taken to be the correct n and k combination.

were relatively independent of wavelength but decreased with increasing working gas pressure, probably because of an increased porosity in the higher pressure coatings.[4] Thus for the chromium oxide case the index decreased from about 2.3 (compared to 2.55 for bulk Cr_2O_3) at 0.13 Pa to about 1.8 at 4 Pa. In the iron oxide case the index decreased from about 2.7 (compared to 3.0 for bulk Fe_2O_3) at 0.13 Pa to about 2.1 at 4 Pa. The extinction coefficient for the sputtered chromium oxide coatings was relatively independent of pressure and increased from about 0.2 to 0.4 over the wavelength range from 700 to 380 nm. The extinction coefficient for the stainless steel oxide coatings was also relatively independent of pressure, and varied from about 0.1 to 0.8 as the wavelength was decreased from 700 to 380 nm.

Approximate solar absorptance measurements were made at Telic for chromium oxide and stainless steel oxide coatings deposited onto aluminum foil, aluminum coated glass, stainless steel and stainless steel coated glass using an International Technology Corporation Wiley Alpha Meter. The coating thicknesses were selected to place the first interference minimum at a wavelength of about 1600 nm. The measured absorptances were typically about 0.74 for the chromium oxide and about 0.71 for the stainless steel oxide.[4]

3.3 Reactive Sputtered Cermet Coatings (Task 2)

Cermet type layers were formed by two reactive sputtering methods using Ar-O_2 as a working gas and chromium and stainless steel as sputtering targets.[4] In one method the discharge current was periodically pulsed to a value which was too large for the rate of oxygen injection, so that a metal rather than a metal oxide was deposited. In the second method the oxygen injection was done on a pulsing basis so that periodically the injection rate was so low that a metal rather than an oxide was deposited.

X-ray diffraction measurements indicate that the coatings deposited with the pulsed O_2 injection consist of crystalline and amorphous phases. In the chromium case the diffraction patterns clearly show metallic chromium, with

crystal sizes as large as about 20 nm and a (110) orientation, along with what appears to be an amorphous CrO phase. In the stainless steel case a NiO phase with crystal sizes in the 12 to 15 nm range is seen, in addition to the same amorphous oxide with Fe_2O_3 type d-spacing that was seen for the pure O_2 sputtering. The results of an ESCA analysis are shown in Table I.

After a review of the results from approximate solar absorptance measurements made on preliminary chromium and stainless steel cermet coatings deposited onto aluminum foil and aluminum coated glass, it was concluded that future work should concentrate on the stainless steel cermet coatings. This selection was a milestone in the project and was based on the fact that the stainless steel and chromium coatings yielded similar solar absorptances and that stainless steel is available in a form suitable for providing low cost sputtering targets for use in large production.

Attempts to form graded cermet deposits by varying the gas-pulse or current-pulse sequence were not successful in producing coatings with solar absorptances (α_H) greater than 0.90 (achieving $\alpha_H \geq 0.90$ and $\epsilon_H(20^oC) \leq 0.1$ was a milestone in the project). Therefore, the stainless steel cermet coatings were used in a configuration of the type shown in Fig. 1 to form selective surfaces. The antireflective layer was reactive sputtered aluminum oxide. Figures 2 and 3 show the hemispherical reflectance spectrum for two representative coatings.* The hemispherical absorptance (α_H) and the hemispherical emittance (ϵ_H) increase with the thickness and/or the metal content of the cermet layer. Thus, in the coatings shown, a 90 nm cermet layer yielded $\alpha_H = 0.90$ and $\epsilon_H(20\ C) = 0.07$, while a 160 nm cermet layer yielded $\alpha_H = 0.94$ and $\epsilon_H(20\ C) = 0.23$. The aluminum oxide layers were in the 70 to 85 nm range.

*These figures are based on so called "distorted- λ plots" that display the reflectance against an abscissa which is linear in fractions of the total solar flux. The total area of the graph therefore corresponds to the total solar flux, and the area above the reflectance curve to the solar absorptance.

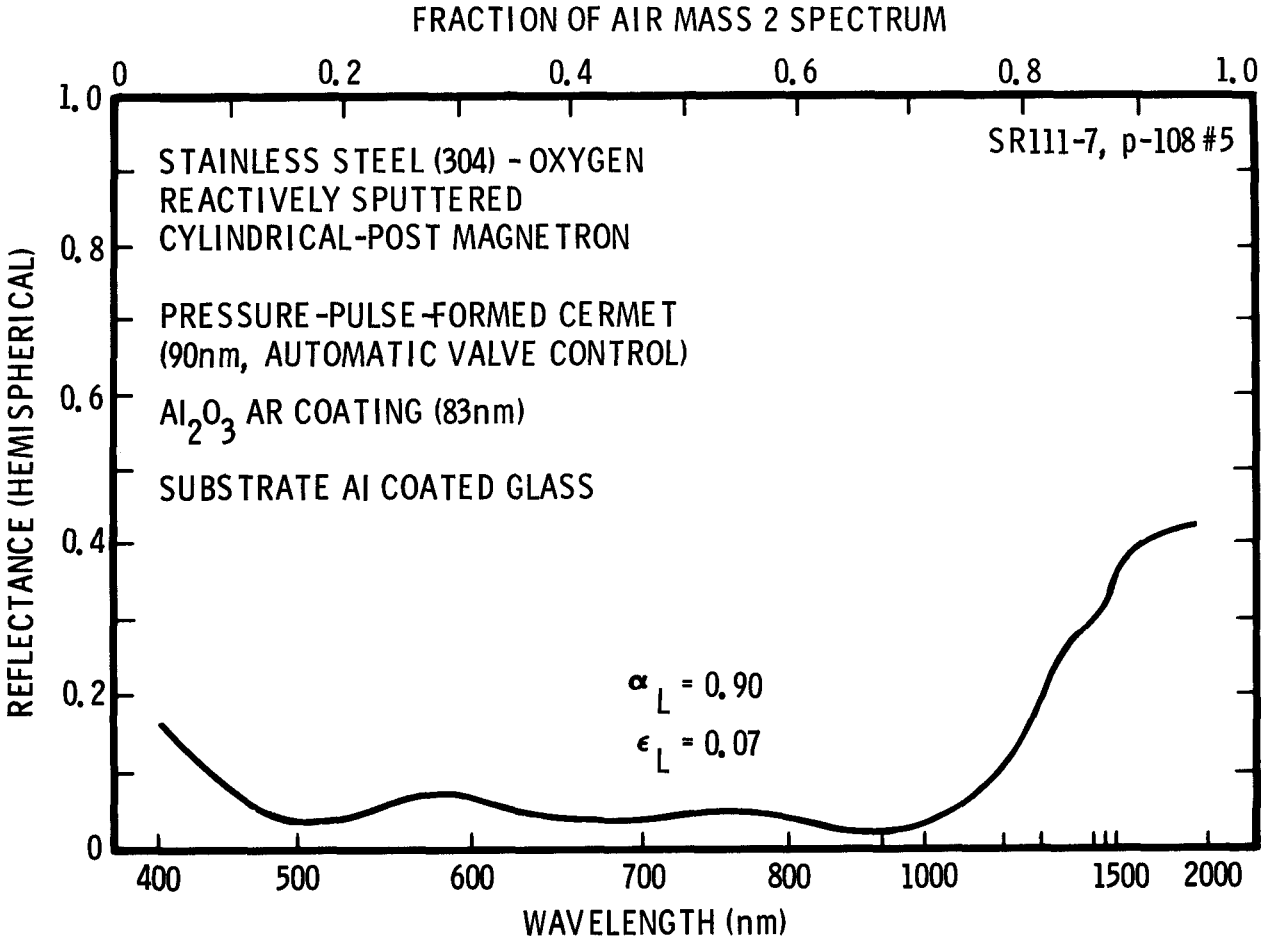

FIG. 2. Hemispherical reflectance vs. wavelength (distored λ plot) for coating with stainless-steel/stainless-steel-oxide cermet absorbing layer and aluminum oxide antireflective layer.

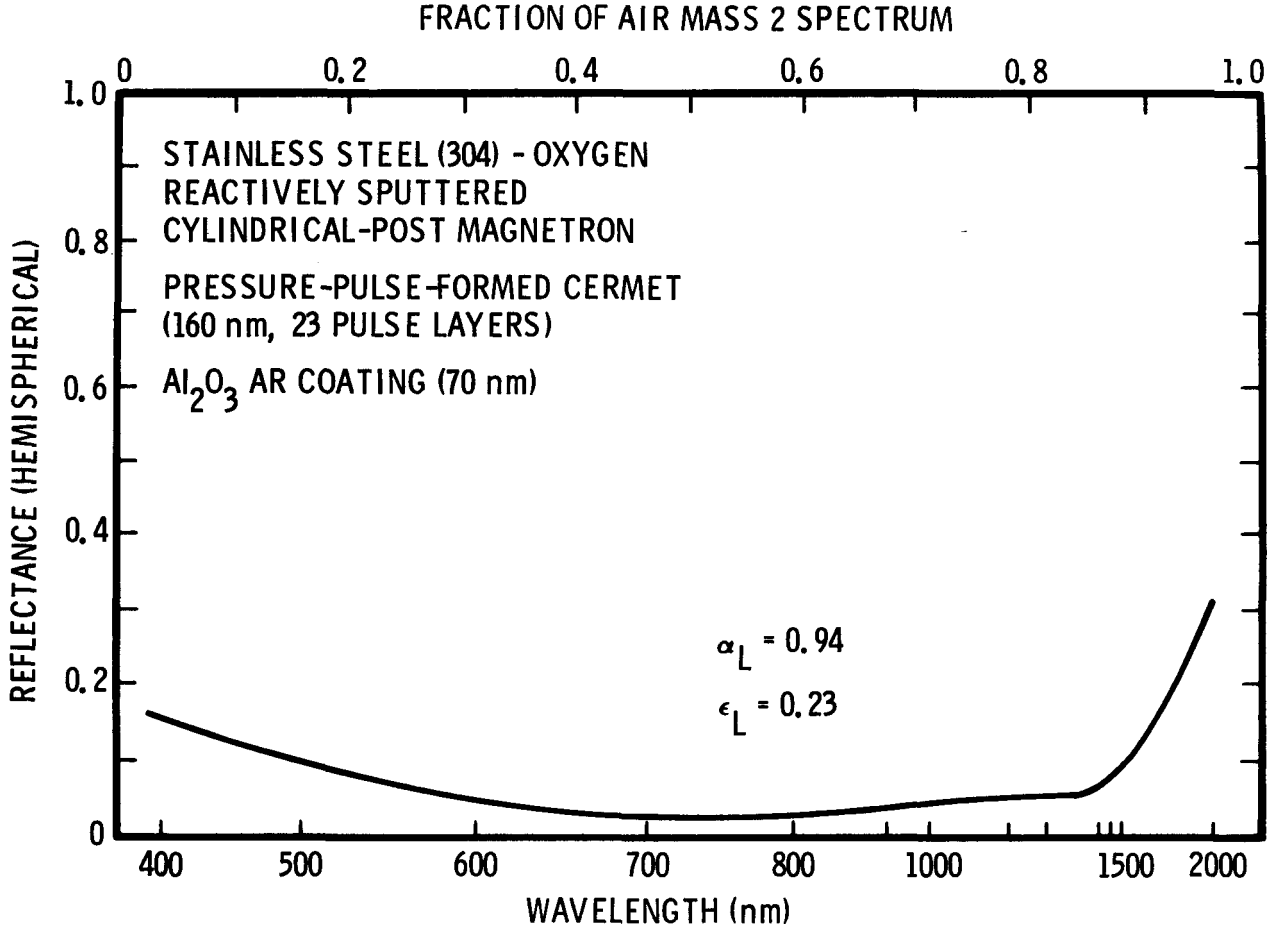

FIG. 3. Hemispherical reflectance vs. wavelength (distorted λ plot) for coating with thick stainless-steel/stainless-steel-oxide cermet absorbing layer and aluminum oxide antireflective layer.

The coatings shown were deposited onto aluminum coated glass substrates. Similar results were obtained on aluminum foil.

The thermal stability of the coatings was examined by heating in air for six hour increments and then testing the optical properties. The coatings were stable in air at 150°C. However, slight changes in absorptance, sometimes increasing and sometimes decreasing, were seen in the range from 200 to 300°C. Thus, the thermal stability of the reactively sputtered coatings appears to be no better than that of electroplated black chromium, which is stable at 250°C but can fail at 300°C.[11,12]

3.4 Reactive Sputtered Stainless Steel-CO Cermets

When stainless steel is sputtered in CO, a dielectric deposit is formed at a deposition rate that is about five times larger than that for stainless steel oxide. Thus the possibility of using this material to form selective surfaces was examined.

X-ray diffraction measurements were made on deposits formed by sputtering type 304 stainless steel in Ar-CO gas mixtures at CO injection rates which provided sputtering conditions just prior to, and just beyond, the point of cathode poisoning.[4] The coatings deposited just prior to the transition were metallic in nature. However, the diffraction pattern was amorphous, with the broad maximum corresponding to a metallic stainless steel diffraction line. The post-transition material was dielectric in nature. It was also amorphous, with a broad low intensity diffraction pattern having a maximum at a point corresponding to a d-spacing of 2.12Å (close to 2.09Å line of stainless steel). This is in contrast to the case of stainless steel sputtered in pure O_2, where the broad amorphous signal is close to the d-spacing (2.70Å) for alpha Fe_2O_3 (see Section 3.2).

ESCA analyses* were made on the metallic and dielectric coatings sputtered in Ar-CO and on comparative coatings sputter-deposited from type 304 stainless

*ESCA (X-ray photoelectron spectroscopy) analyses were made at Surface Science Laboratories, Inc., Palo Alto, CA. The analyses were made after argon ion etching the samples for 30 min to remove surface contamination.

steel targets in pure O_2, and in Ar-O_2 with pulsed O_2 injection, as described in the preceding section. The results are summarized in Table I. The relative N, Ni, Cr and Fe contents are the same for all of the samples within experimental error. The relative oxygen content is highest for the samples sputtered in O_2 and lowest for the metallic coating sputtered in Ar and CO, as would be expected. Similarly, the relative carbon content is highest for the sample sputtered in pure CO. Thus sputtering with CO does indeed introduce carbon into the deposits.

Measurements of n and k as a function of wavelength were made for the dielectric material formed by sputtering stainless steel in pure CO at 1.13 Pa. The n and k values were determined from transmission and reflectance measurements, as described in Section 3.2. Over the wavelength range examined (350 to 700 nm), the index of refraction was about two and the extinction coefficient varied between 0.3 and 0.4.[4]

Selective absorber coatings of the configuration shown in Fig. 1 were deposited using the metallic pre-transition material sputtered in Ar+CO as the absorbing base layer and the dielectric material sputtered using pure CO as the antireflective layer. The metallic layers were deposited at a rate of about 1 nm/s using a current density of 8 mA/cm^2 and a voltage of 900V. The dielectric layers were deposited at a rate of about 0.6 nm/s using a current density of 8 mA/cm^2 and a voltage of 700V. The absorbing base layer was typically 40 nm thick. Figure 4 shows the effect of the dielectric antireflecting layer thickness on the spectral reflectance of the coatings. An absorptance of 0.89 and an emittance (20°C) of 0.08 were obtained for a dielectric thickness of 80 nm. The coatings shown were deposited on aluminum coated glass. Similar results were obtained for aluminum foil substrates.

The thermal stability of the coatings was examined by heating in air for six hour increments and then testing the optical properties. The coatings were stable in air at 150°C. However, changes in absorptance were seen at 200°C.

TABLE I

ESCA Analysis of Coatings Sputtered from Type 304 Stainless Steel Targets with Various Working Gases.

	Pure O_2	$Ar+O_2$ Pulsed O_2 injection	Pure CO (post-transition)	Ar+CO (pre-transition)
C	1.3	0.71	4.0	1.0
O	3.9	3.7	2.2	1.2
N	0.11	0.14	0.11	0.13
Ni	0.06	0.06	0.08	0.07
Cr	0.37	0.36	0.34	0.31
Fe	1.00	1.00	1.00	1.00

Relative number of atoms for the detected elements compared to Fe (atom ratios).

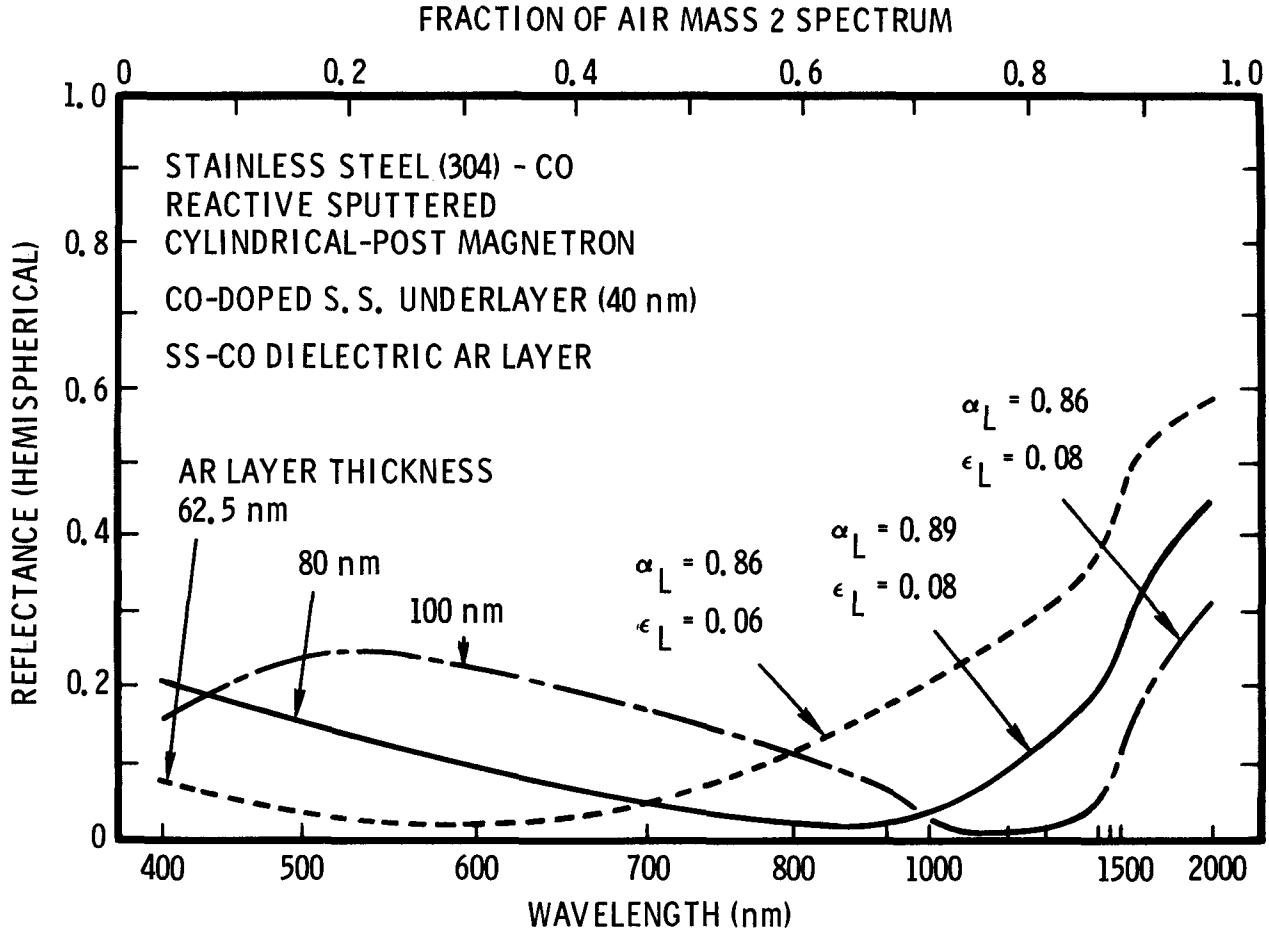

FIG. 4. Hemispherical reflectance vs. wavelength (distored λ plot) for coatings with stainless-steel/CO metallic abosrbing layer and stainless-steel/CO dielectric surface layers of various thicknesses.

3.5 Dual Source Deposition of Cermet Coatings (Task 3)

Dual source deposition is of interest because it permits cermets with graded metal compositions to be deposited. A cermet can be formed by reactive sputtering from two sources in a common or near common reactive gas if the cermet metal component is relatively inert to the reactive gas. Thus cermets of the type being investigated on the present program, such as Cr-Cr_2O_3 and Cr-Al_2O_3, are difficult to deposit by dual source reactive sputtering.[4] Accordingly, Cr-Al_2O_3 cermet deposits with graded Cr-contents were formed by simultaneous sputtering from Al_2O_3 (using rf power) and Cr cylindrical magnetron sputtering sources. Al_2O_3 deposition rates were about 0.02 nm/s. Cr deposition rates were varied between 0.2 nm/s and zero to produce the grading. The apparatus used in this work is described in Section 4.3.

Typical coatings consisted of 100 nm thick Al_2O_3 layers deposited onto aluminum coated glass substrates with Cr contents which varied from about 50 atomic percent at the rear surface to zero over the first 50 nm of the coating. Figure 5 shows an Auger depth profile* of one of the coatings, demonstrating the degree to which the Cr composition can be controlled and graded by the sputtering process.

Figure 6 shows the hemispherical reflectance versus wavelength for two of the Cr-Al_2O_3 coatings. The Auger data in Fig. 5 are for the coating with an absorptance of 0.92 and an emittance of 0.09. No attempt was made to optimize the performance of these coatings. The objective was simply to demonstrate the capabilities of the magnetron sputtering process.

4. PHASE 2 - Al_2O_3-Mo-Al_2O_3 COATINGS

4.1 Background Considerations

The original AMA coatings were developed for a high temperature spaceborne application and are known for their thermal stability.[13] Coatings with solar absorptance of 0.83 and total emittances of 0.11 at 540°C were deposited

---

* The Auger analyses were made at Surface Science Laboratories, Inc., Palo Alto, CA.

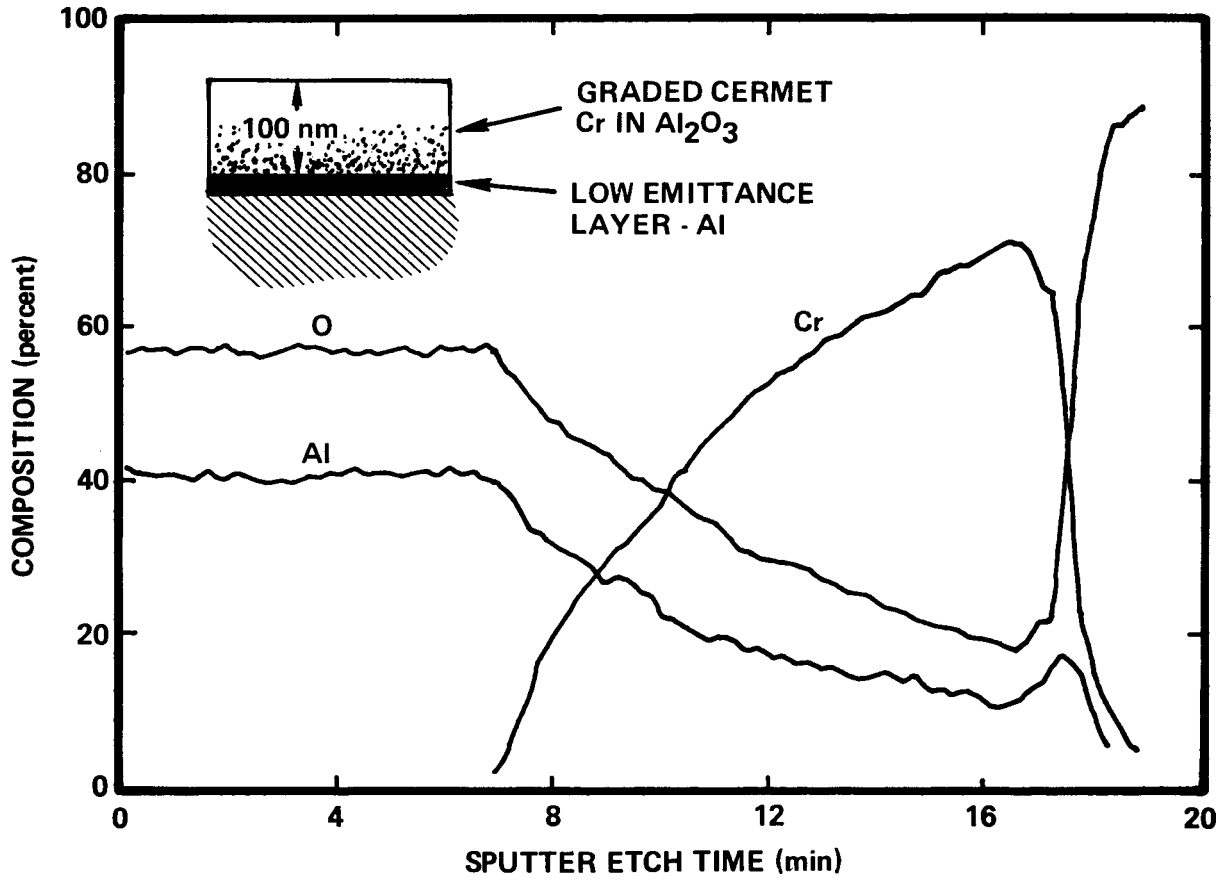

FIG. 5. Auger depth profile composition analysis of Cr/Al_2O_3 cermet with graded Cr composition which was formed by co-sputtering from Al_2O_3 and Cr sources.

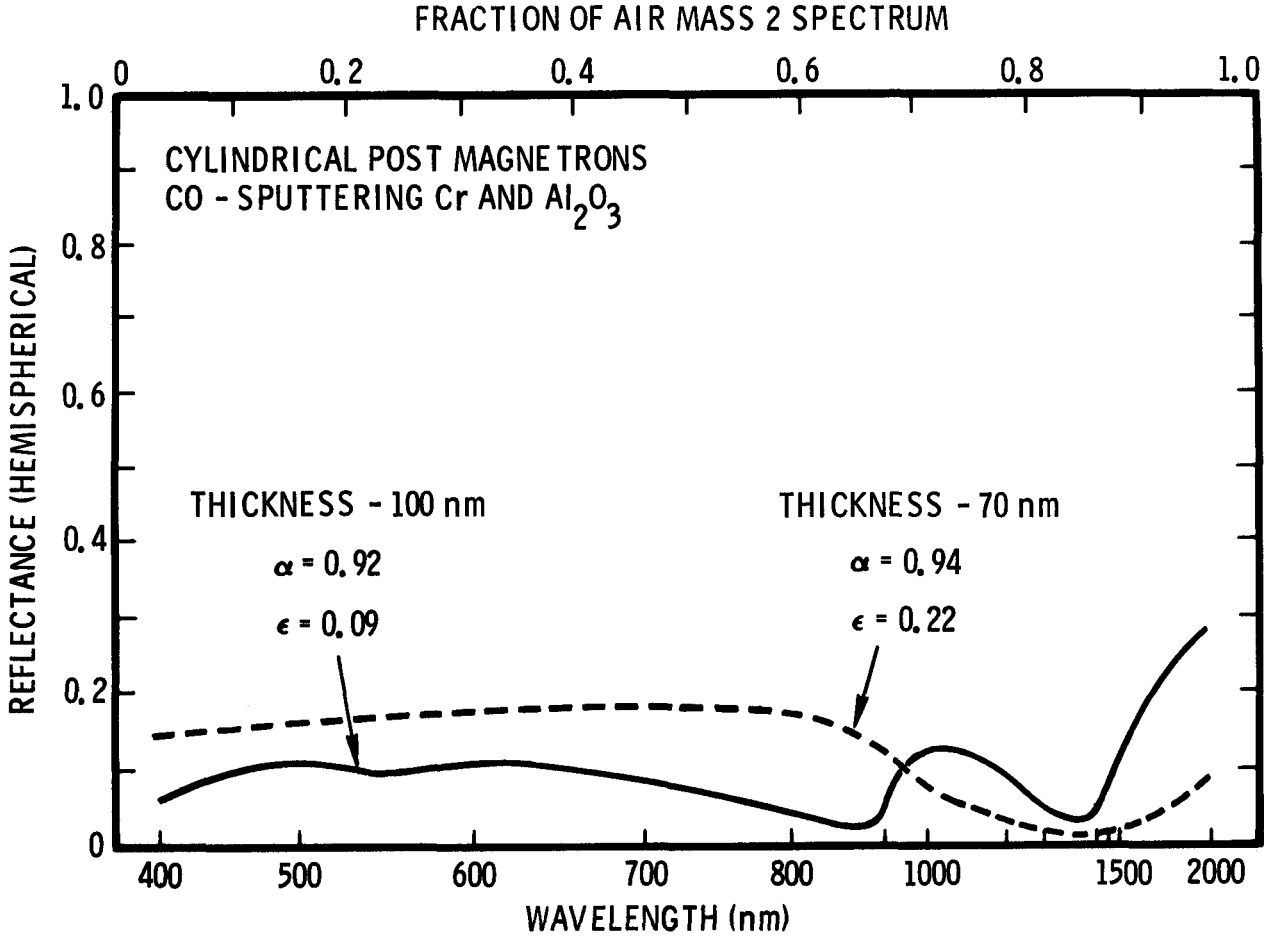

FIG. 6. Hemispherical reflectance vs. wavelength data for Cr/Al_2O_3 cermets with graded Cr composition which were formed by co-sputtering from Al_2O_3 and Cr sources.

by evaporation onto Mo substrates.[13] These coatings were stable (no loss in absorptance) in vacuum at 920°C (500 hrs) but failed at ~1050°C.[14,15] When deposited on Mo-coated stainless steel, they failed at ~900°C because of diffusion of Fe and Cr out of the stainless steel. The coatings survived at least 24 hrs at 400°C in air.[16] AMA coatings with absorptances of 0.8-0.9 and emittances of 0.07-0.10 at ~150°C have also been reported.[17] Despite their impressive thermal properties, the use of AMA coatings has been plagued by the difficulty of preparation by vacuum evaporation.[16]

The objective of the Phase 2 investigation was to examine AMA coating deposition by sputtering.

4.2 Theoretical Coating Design Studies

In the case of the evaporated AMA coatings, it was found that the best performance was obtained when the Mo layer was deposited with a small amount of O_2 injected into the chamber. In the Telic work this behavior was examined by determining the optical constants (n and k) for Mo sputter-deposited in Ar and in Ar with injected O_2 [this material will be referred to as Mo(0)] over the wavelength range from 400 to 1800 nm. Oxygen injection rates were in the range 0 to 28 scc/min. The optical constants were determined from transmission and reflectance measurements, made on thin (30 to 60 nm thick) single layer films of these materials, using a set of curves provided by Hadley[10] (see discussion in Section 3.2). Typical Mo and Mo(0) (n and k) data are shown in Fig. 7. For wavelengths less than 1000 nm, the n values are consistent with previous reported data, although the k values are lower than those previously reported.[18] The injected O_2 is seen to decrease the magnitude of the extinction coefficient, particularly at large wavelengths where the index of refraction is also reduced so that the overall effect is to reduce the wavelength dependence of the Mo(0) optical constants.

Similar measurements were made for reactive sputtered aluminum oxide over the wavelength range from 400 to 700 nm. These measurements yielded $n \sim 1.7$ and $k \sim 0$, consistent with accepted values.[19]

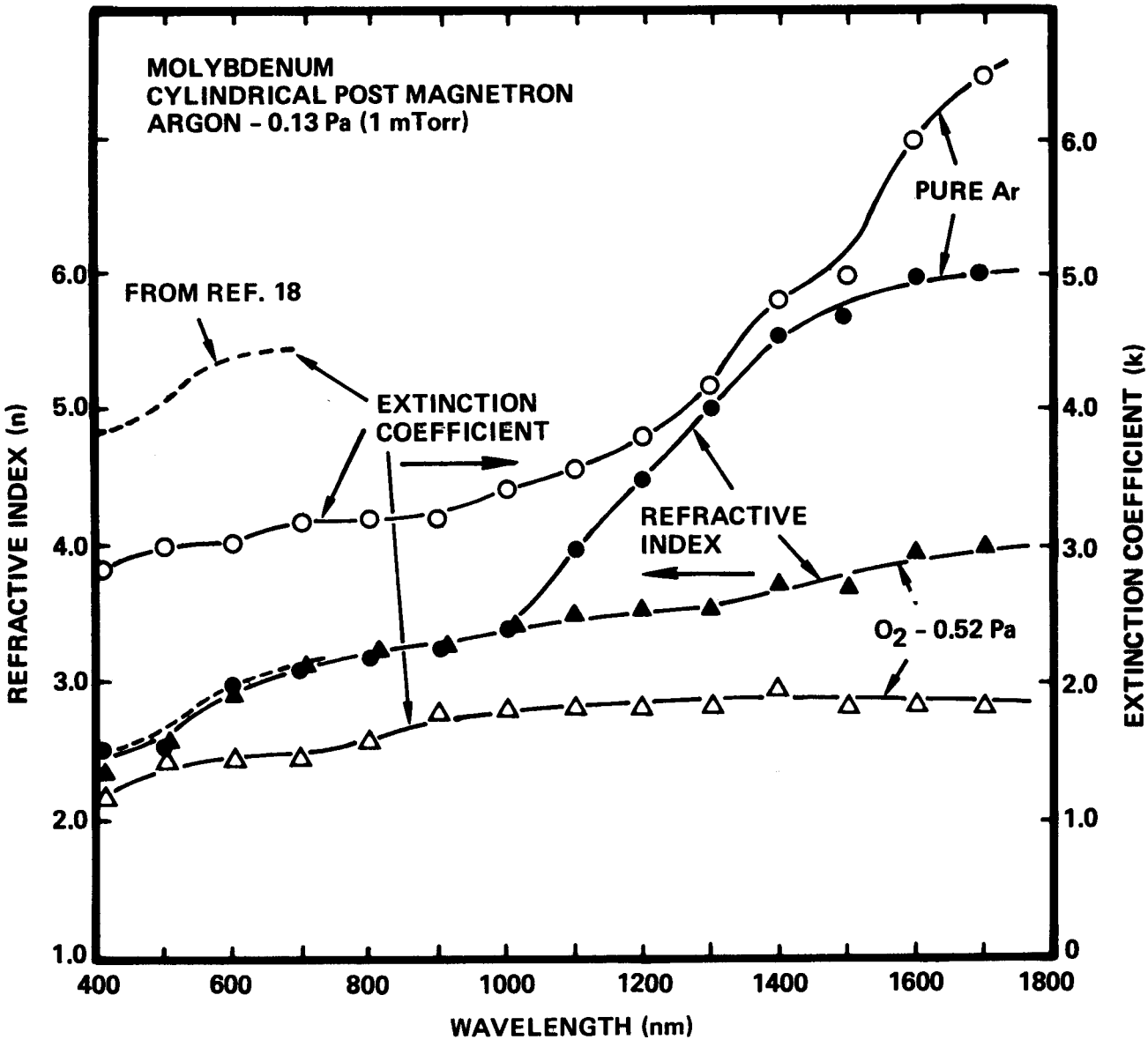

FIG. 7. Optical constants for molybdenum coatings sputter-deposited with pure argon and with argon-oxygen mixture (O_2 injection rate 23 scc/min).

The measured n and k values were used in a theoretical analysis designed to provide insight into the influences of the various coating layers on the AMA optical properties and to predict thickness combinations that would provide low reflectances $r(\lambda)$ and high absorptances. Solar absorptances were calculated from the following relationship

$$\alpha = \frac{\int_0^\infty [1-r(\lambda)]\, E(\lambda) d\lambda}{\int_0^\infty E(\lambda) d\lambda} \qquad (1)$$

where $E(\lambda)$ is the air mass two spectral solar energy distribution (SERI SOLTRAN spectrum, available from Solar Energy Research Institute, Golden, CO). Several combinations of coating thicknesses were found in to yield $\alpha \sim 0.95$. Typical top-to-substrate AMA thicknesses were about 70 nm/8 nm/70 nm for a Mo intermediate layer, and about 90 nm/20 nm/50 nm for a Mo(0) intermediate layer. The AMA coatings with Mo(0) intermediate layers were found in the experimental work to yield higher α/ϵ than those with Mo intermediate layers. This behavior is attributed to the role of oxygen in reducing the Mo(0) n and k values at long wavelengths. Optimum thicknesses of about 60 nm/20 nm/30 nm are reported for the evaporated Al_2O_3-Mo(0)-Al_2O_3 coatings.[20]

Figure 8 shows a type of diagram which was used to expose the influence of the various layers in the AMA coating. The diagram plots the real (x-axis) and imaginary (y-axis) parts of the optical reflection coefficient, defined as the ratio of the electric field strength in the electromagnetic wave passing out of the surface to that of the wave passing into the surface in question. Thus starting at "A" with a set of points which represents the reflectance at various wavelengths for a freshly deposited Mo surface, one finds that these points are translated around the large circles to B as the base Al_2O_3 thickness is increased. The Al_2O_3 coatings move the reflectance points on circles because the extinction coefficient is near zero. By contrast, the Mo or Mo(0) layers, with their relatively high extinction coefficients, move

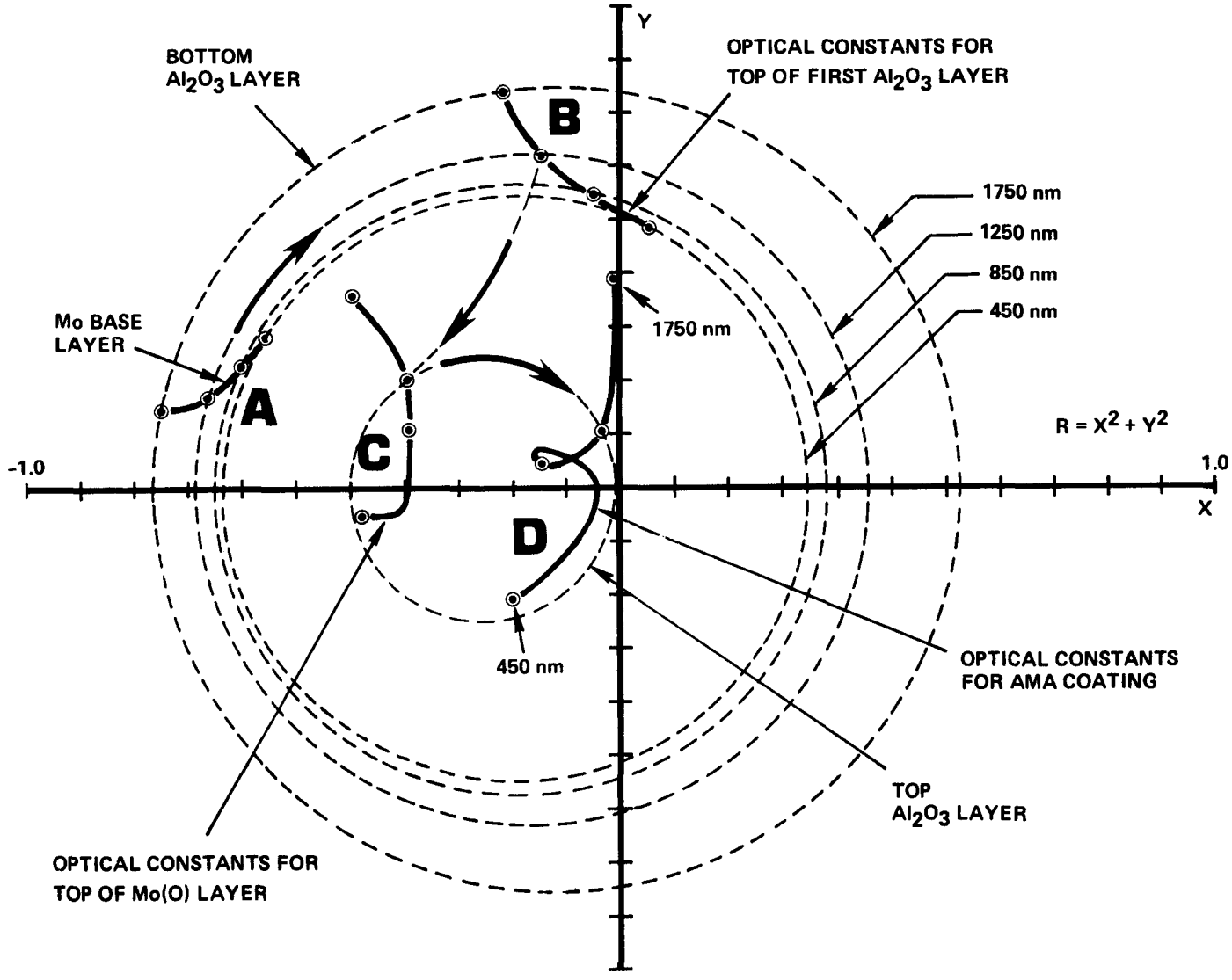

FIG. 8. Diagram giving optical properties of coating layers as a function of the real (x-axis) and imaginary (y-axis) components of E^-/E^+, where E^+ is the electric field strength in the incident electromagnetic wave and E^- is the field strength in the reflected wave.

the locus of reflectance points from B to C in complex paths. Finally, the circles corresponding to the top Al_2O_3 layer (shown only for wavelength of 1250 nm) move the reflectance points to D. The points at D represent the top surface reflectance. The reflectance is proportional to the square of the distance from the origin to a point in question. The goal is therefore to get those particular points which correspond to solar flux wavelengths to be as close as possible to the origin. It is seen that this has been accomplished for the case shown. Figure 9 shows the reflectance versus wavelength, illustrating the accumulating effects of the various layers for the case shown in Fig. 8.

4.3 Coating Deposition

The AMA coatings were deposited in a chamber which mounted two cylindrical-post magnetron sputtering sources as shown in Fig. 10. One magnetron contained a 3.8 cm dia x 30 cm long Mo target machined from commercial rod stock (Teledyne Wah Chang, Huntsville, AL). The Al_2O_3 layers were deposited from the other source by dc reactive sputtering from a 7.6 cm dia x 30 cm long 99.99% Al target, and by rf sputtering from a 6.3 cm dia x 30 cm long alumina target (type AD-94*, Coors Porcelain Co., Golden, CO) driven single ended at 1.8 MHz with the chamber walls grounded and the substrates electrically floating.

The chamber was evacuated to about 10^{-3} Pa prior to deposition using a freon-trapped oil diffusion pump (90 l/sec for air). The Mo coatings were deposited using Ar working gas at 0.2 Pa (measured with a capacitive manometer) and with O_2 injection at rates of from 0 to 28 scc/m. The rf sputtered Al_2O_3 coatings were deposited using Ar at 0.2 Pa. The reactive sputtered Al_2O_3 coatings were deposited using pure O_2 at pressures of from 0.13 to 1.3 Pa. Deposition rates were determined under various deposition conditions by interferometrically measuring steps in coating thickness that were formed on

*94% Al_2O_3; residual is SiO_2, MgO and CaO.

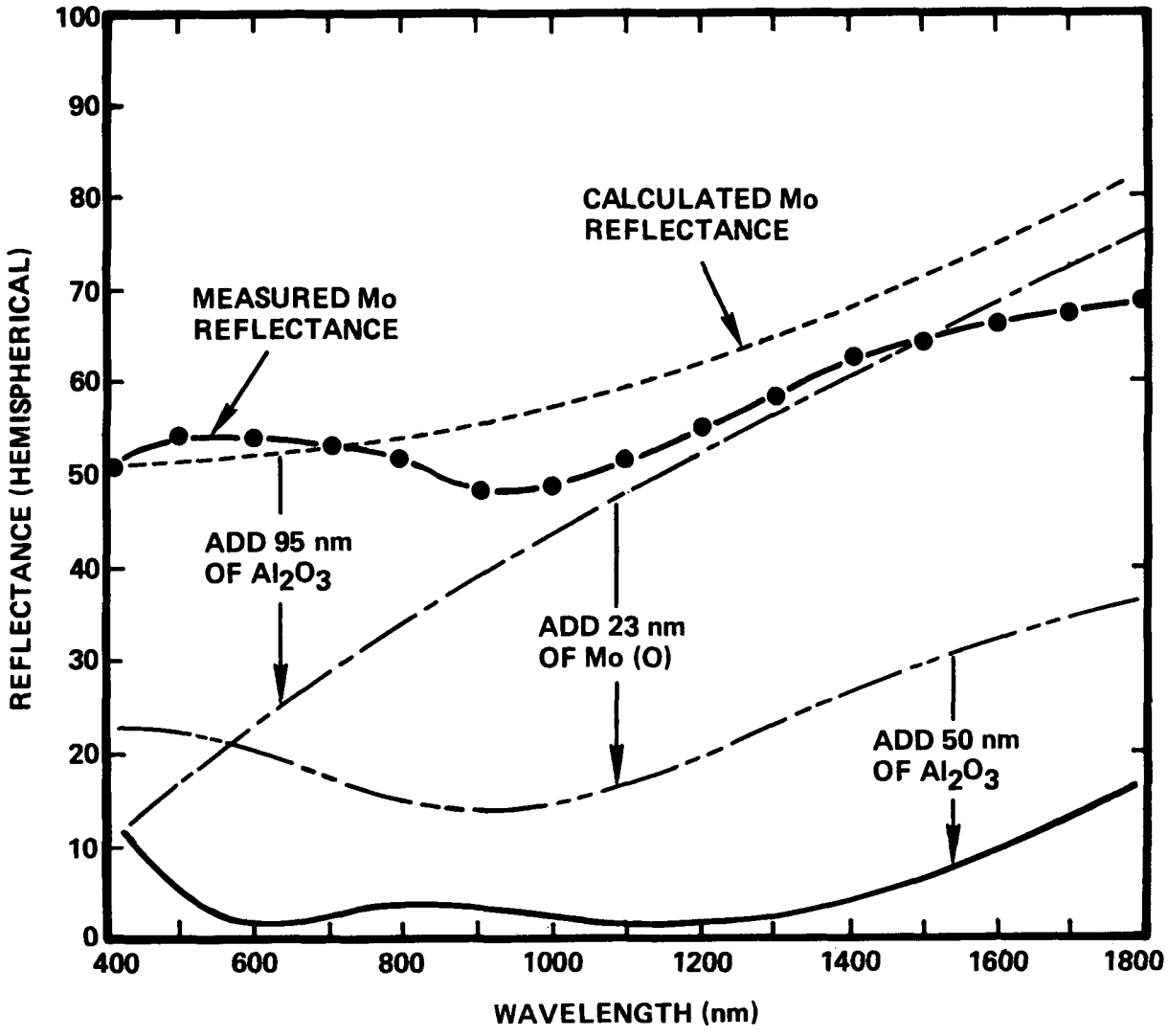

FIG. 9. Results of theoretical calculation showing the influence of the various Al_2O_3 and Mo(0) layers in reducing the reflectance over the wavelength range of the solar spectrum.

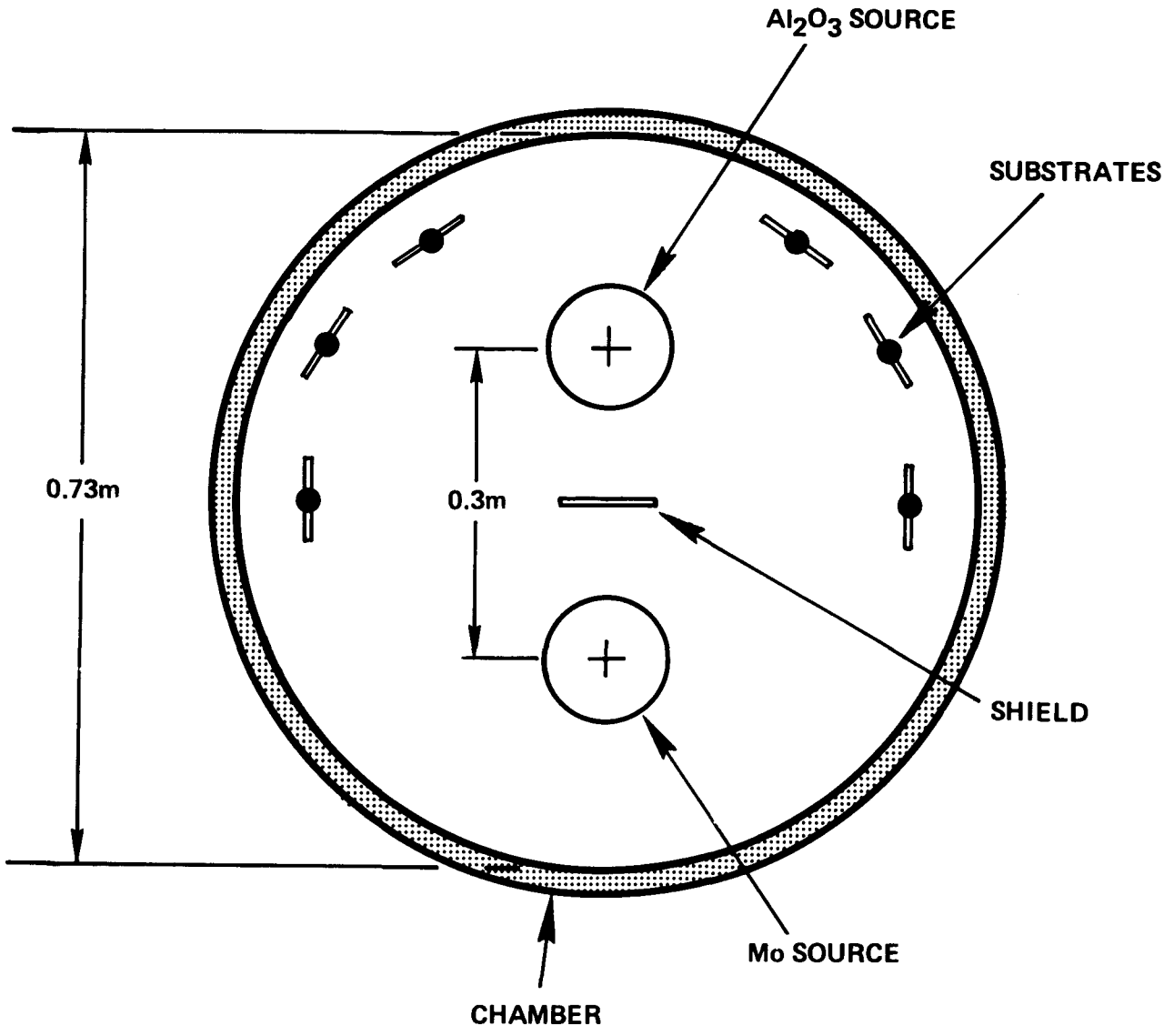

FIG. 10. Schematic illustration showing arrangement of cylindrical-post magnetrons in apparatus which was used to deposit Al_2O_3-Mo-Al_2O_3 coatings.

glass substrates using masks. The Mo deposition rate was typically 0.13 nm/s. The Al_2O_3 deposition rates were about 0.06 nm/s for the rf sputtered coatings and about 0.02 nm/s for the reactive sputtered coatings.

The AMA coatings were deposited with specified layer thicknesses by controlling the deposition times. The substrates were glass (soda lime) and type 304 stainless steel (SS) plates (typically 50 mm x 50 mm x 2 mm). In all cases an 80 nm thick Mo base layer was deposited onto the substrates to provide a low emittance starting surface. On some of the stainless steel substrates an rf sputtered alumina diffusion barrier 50 nm thick was deposited prior to depositing the Mo base layer.

All substrates were degreased in trichloroethylene and rinsed in isopropyl alcohol prior to deposition. In addition, the SS was dc sputter-cleaned in Ar(2 Pa) at 1 mA/cm^2 and 800V for 5 min. The cathodes were operated at a current density of $\sim$10 mA/cm^2 for 5 min prior to deposition, with the substrates shielded. Similar current densities were used during deposition. During deposition, the substrates were oriented to receive coating flux at a generally normal angle of incidence. In most cases the substrates were mounted on thermally isolated substrate holders. Substrate temperatures are estimated to have been less than 100°C.[21] In selected cases coatings were deposited on heated substrates at temperatures in the 200°C to 400°C range.

Additional coatings were deposited onto flat plate substrates using the in-line hollow cathode system, shown schematically in Fig. 11, in anticipation of the Phase 4 proof-of-concept experiments (see Section 6). The system was configured to incorporate a dc-driven Mo target and a double ended rf-driven Coors AD-94 alumina target. The AMA coatings deposited with this apparatus had pure Mo intermediate layers. The Mo was deposited at $\sim$0.15 nm/s using Ar at 0.4 Pa; the Al_2O_3 at $\sim$0.1 nm/s using Ar at 0.12 Pa.

4.4 Coating Optical Properties

The optical properties of the AMA coatings were in general agreement with the theoretical predictions. See Fig. 12. The optical properties were inde-

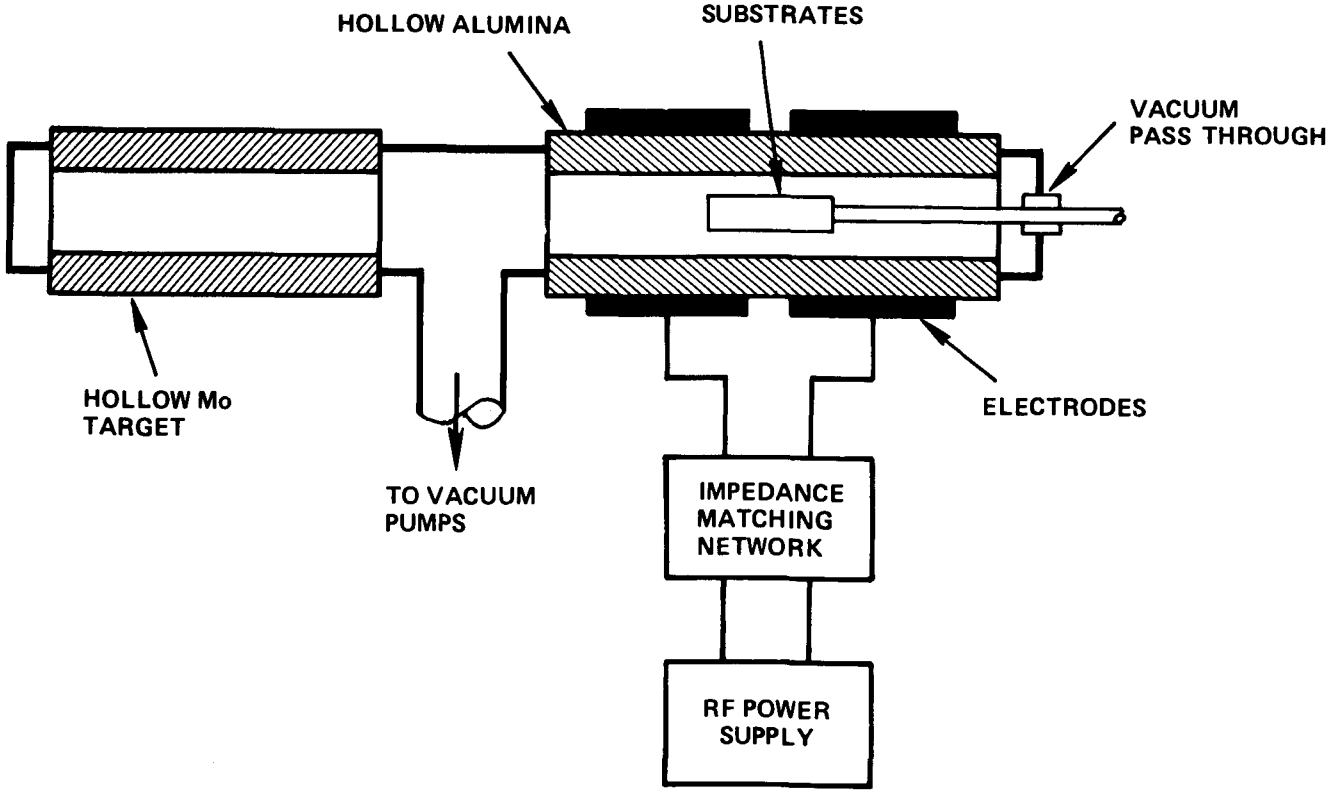

FIG. 11. Schematic illustration showing arrangement of cylindrical-hollow magnetrons on in-line apparatus used to deposit Al_2O_3-Mo-Al_2O_3 coatings.

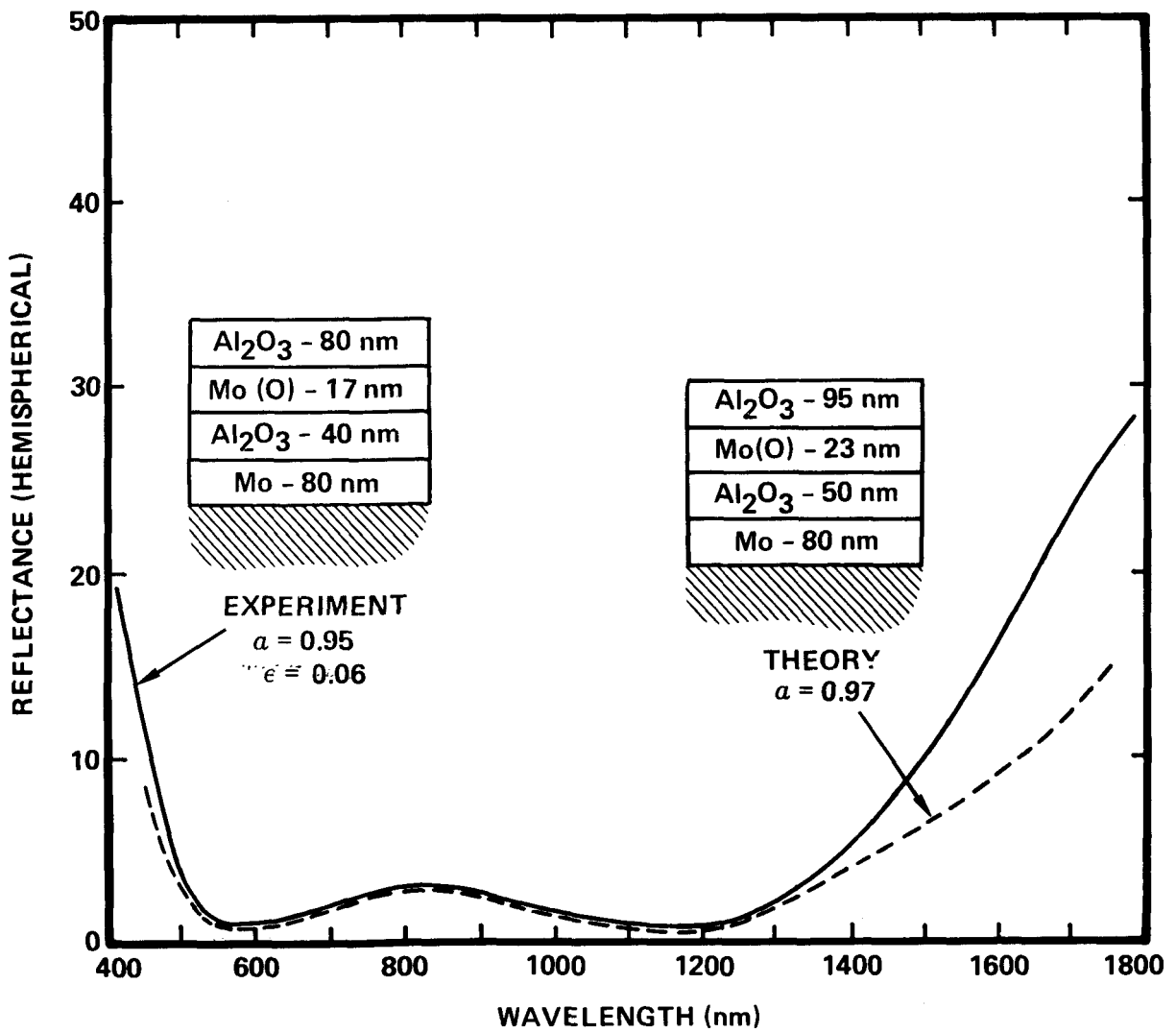

FIG. 12. Comparison between theory and experiment for Al_2O_3-Mo-Al_2O_3 coatings.

pendent of whether the Al_2O_3 layers were deposited by reactive or direct rf sputtering or by using post or hollow cathodes. However, the nature of the molybdenum intermediate layers did have an effect. Lower emittances were obtained with the coatings having Mo(0) intermediate layers. This is believed to be due to the lower long wavelength extinction coefficients for the Mo(0) coatings, as discussed in Section 4.2. Thus, post magnetron coatings with α_H = 0.94-0.95 and ϵ_H = 0.06-0.07 (20°C) were obtained with Mo(0) intermediate layers. The best coatings with Mo intermediate layers were post magnetron coatings with α_H = 0.90-0.92 and $\epsilon_H \sim 0.10$, and hollow cathode coatings with α_H = 0.94 and $\epsilon_H \sim 0.20$. Superior optical properties (α, ϵ) were also reported in the evaporation work for coatings deposited using Mo(0) semitransparent layers.[20]

The coatings could tolerate ± 15% thickness variations within the layers with little change in α_H and ϵ_H. Variations in the Al_2O_3 oxygen deposition pressure over the range from 0.13 to 1.3 Pa, and in the substrate temperature over the range 100 to 400°C, were found to have little effect on the absorptance of AMA coatings with reactively sputtered Al_2O_3 layers.

4.5 Coating Thermal Stability

Sample Al_2O_3-Mo-Al_2O_3 coatings on type 304 stainless steel substrates were tested for 6 hrs each at increasing temperatures with 50° to 100°C increments starting at 300°C, in both air and vacuum (7.5×10^{-3} Pa). Measurements of solar absorptance and emittance were made after each 6 hr test using an International Technology Corporation Wiley Alpha Meter and Ambient Emissometer.

The results of these tests are summarized in Fig. 13. The thermal stability of the AMA coatings, with Al_2O_3 layers deposited using direct rf sputtering from an alumina target, was superior to that of coatings with reactively sputtered Al_2O_3. Coatings with reactive-sputtered Al_2O_3 and Mo or Mo(0) intermediate layers were stable to 300°C in air but failed (2% loss in

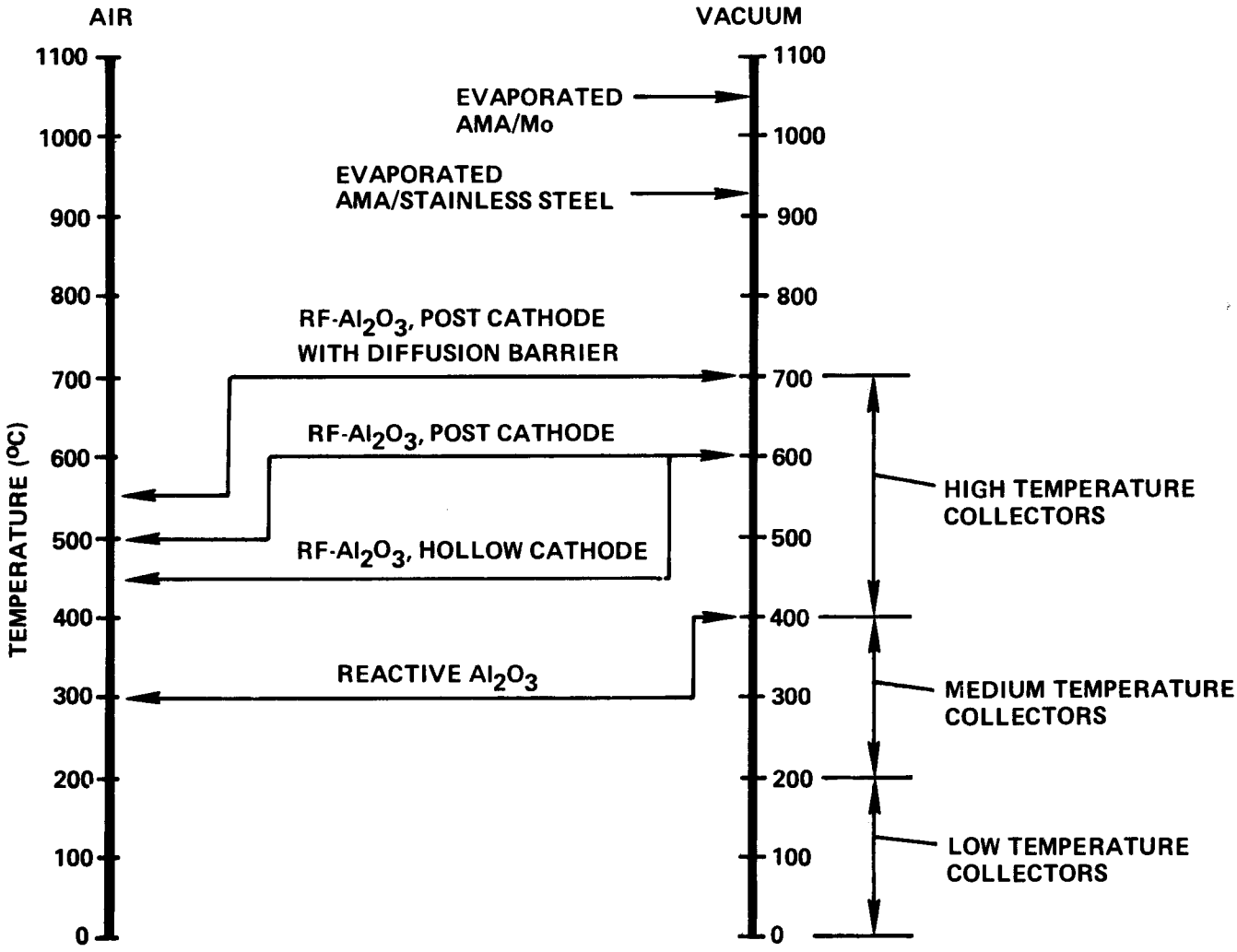

FIG. 13. Summary of thermal stability data for sputter deposited Al_2O_3-Mo-Al_2O_3 coatings.

α_H) at 400°C. In vacuum they were stable at 400°C but failed at 500°C (see Fig. 14). For convenience in deposition, the coatings with the rf sputtered Al_2O_3 all had pure Mo intermediate layers. The hollow cathode coatings did not have Al_2O_3 diffusion barriers. These coatings were stable at 450°C in air (141 hrs) but failed at 500°C. The post cathode coatings (less oblique coating flux), with rf sputtered Al_2O_3 but no diffusion barriers, were stable in air at 500°C and failed at 550°C. In vacuum both of these types of coatings were stable at 600°C but failed at 650°C. Post cathode coatings, with rf-sputtered Al_2O_3 layers forming the AMA stack and a 50 nm rf-sputtered Al_2O_3 diffusion barrier between the stainless steel and the Mo base layer, showed no loss in α_H at 700°C during vacuum tests which lasted 12 hrs. These coatings were stable in air at 550°C during tests which lasted 14 hrs.

Auger depth profiling revealed the failure mechanisms. The low temperature failure of the coatings with reactively sputtered Al_2O_3 was due to a diffusion breakdown of the AMA layers. This is seen in Fig. 15. The Mo intermediate layer is distinct and clearly apparent in the as-deposit coating (15a) but totally intermixed after heat treatment at 500°C in vacuum (15b).

The improved performance of the coatings with the direct rf sputtered Al_2O_3 apparently resulted because this form of Al_2O_3 provides a superior diffusion barrier. This is seen in the depth profile data shown in Fig. 16a. Massive breakdown on the AMA layers is not apparent after heat treatment at 800°C. Fe and Cr diffused completely and intermixed with the thin Mo base layer (high solubility for Cr and Fe) but were largely blocked by the Al_2O_3. However, even this diffusion was sufficient to reduce α_H from 0.94 to 0.82.

The data in Fig. 16b clearly show the effectiveness of an Al_2O_3 diffusion barrier between the stainless steel substrate and the Mo base layer. No evidence of Cr or Fe penetration through the diffusion barrier and into the Mo base layer is seen after 12 hrs at 700°C. Optical measurements indicated no loss in absorptance.

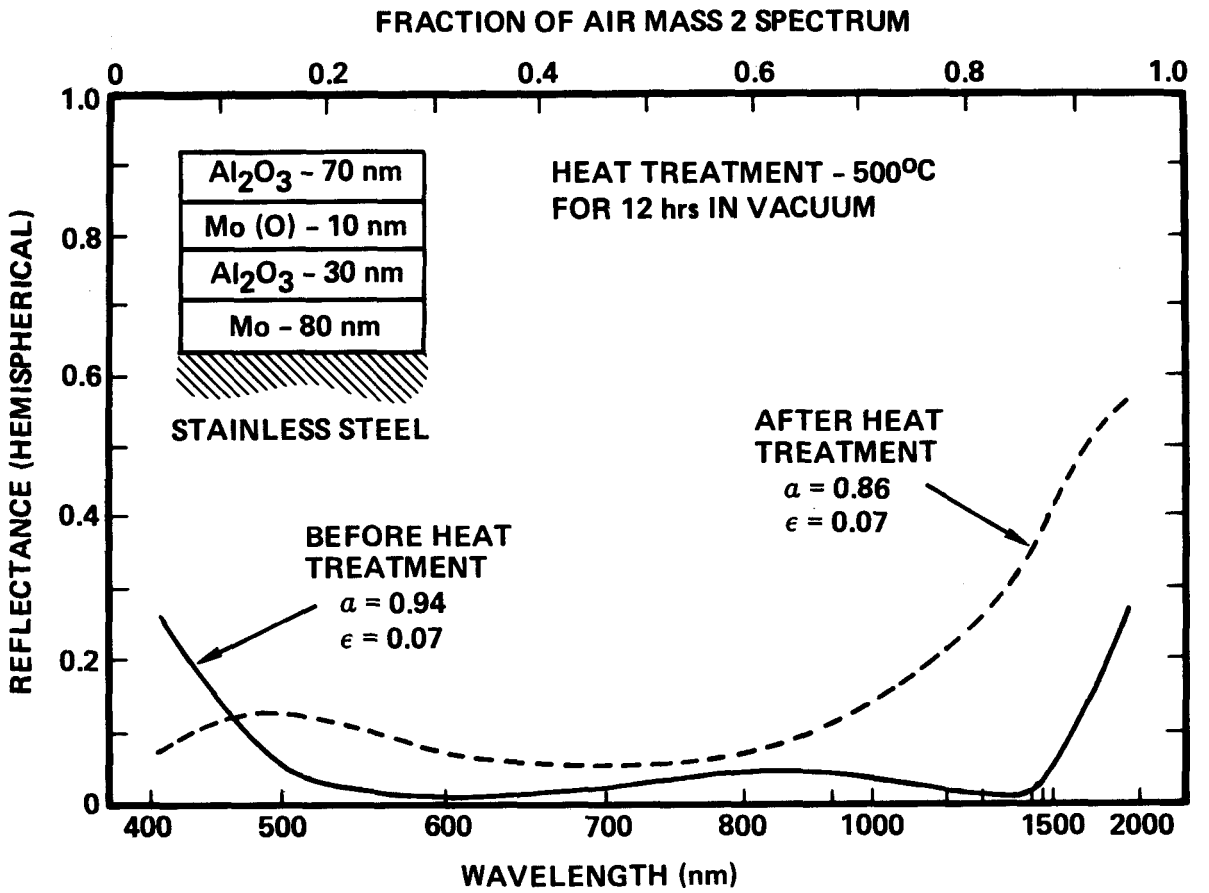

FIG. 14. Change in optical properties of Al_2O_3-Mo(O)-Al_2O_3 coating on Mo-coated stainless steel after heat treatment for 12 hrs at 500°C in vacuum. Al_2O_3 layers formed by reactive sputtering.

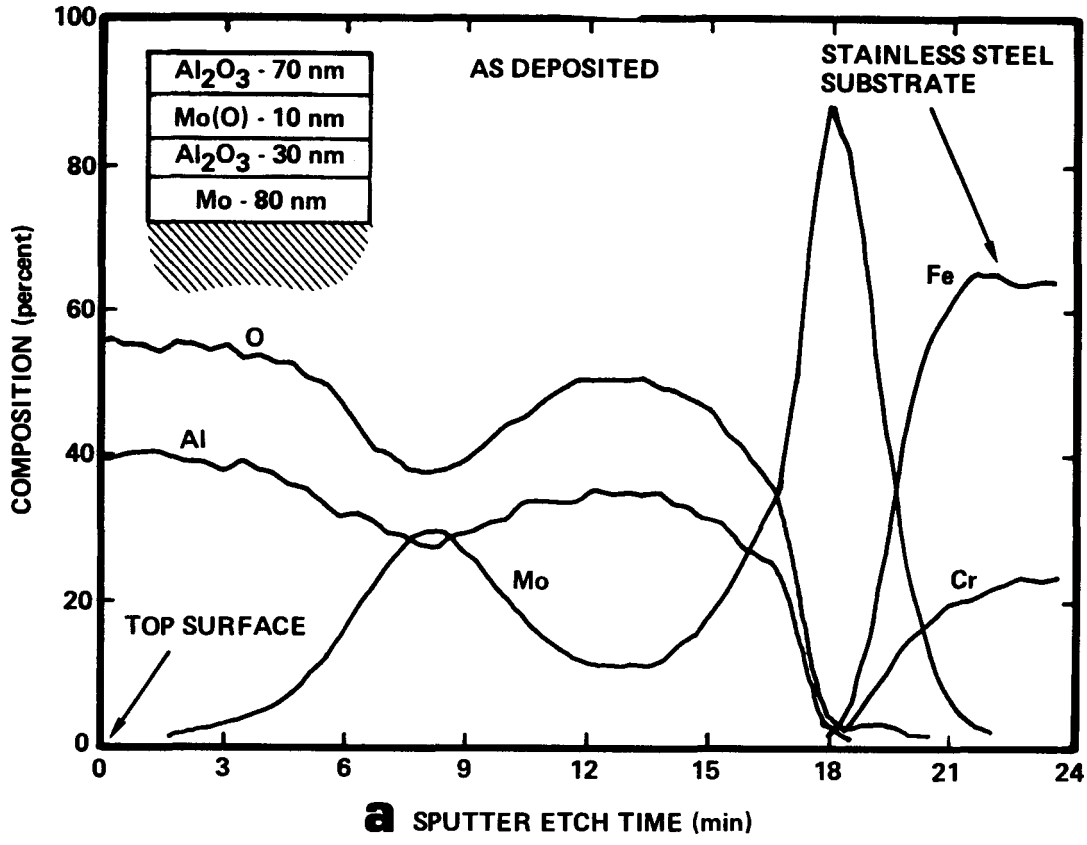

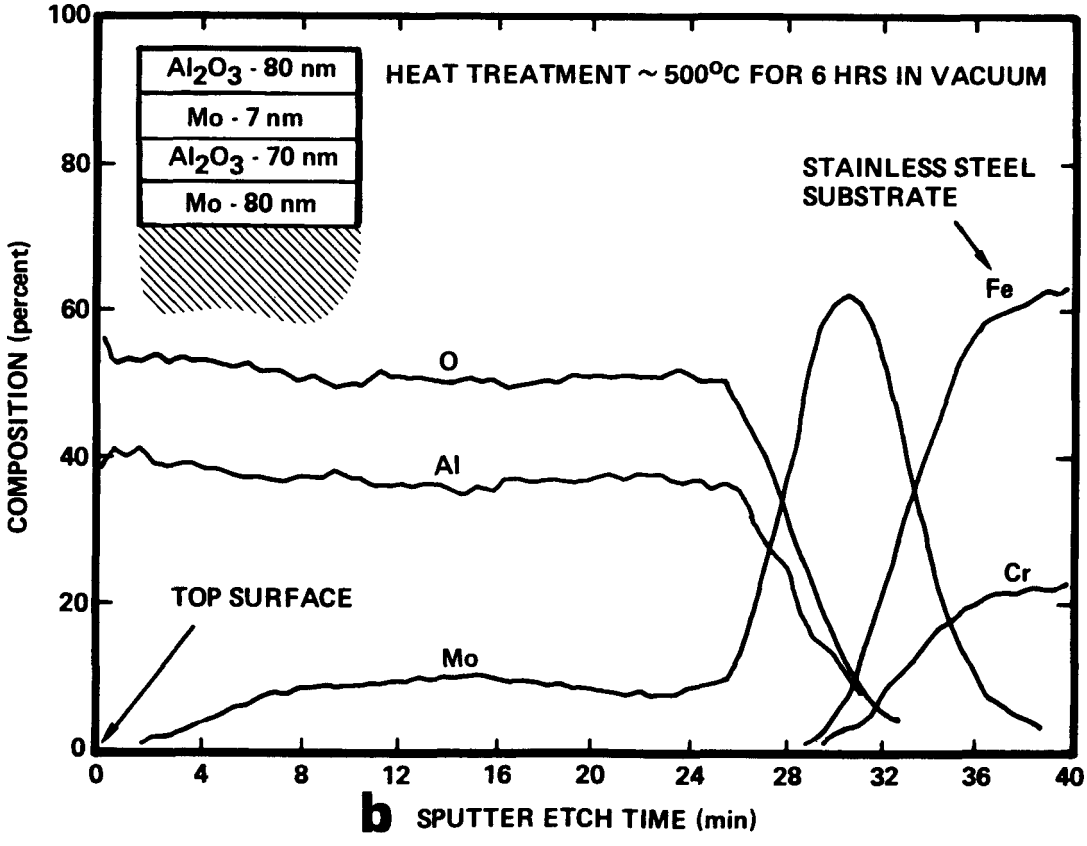

FIG. 15. Auger depth profile composition analyses of Al_2O_3-Mo-Al_2O_3 coatings on Mo coated stainless steel showing effect of heat treatment. The Al_2O_3 layers were formed by reactive sputtering.

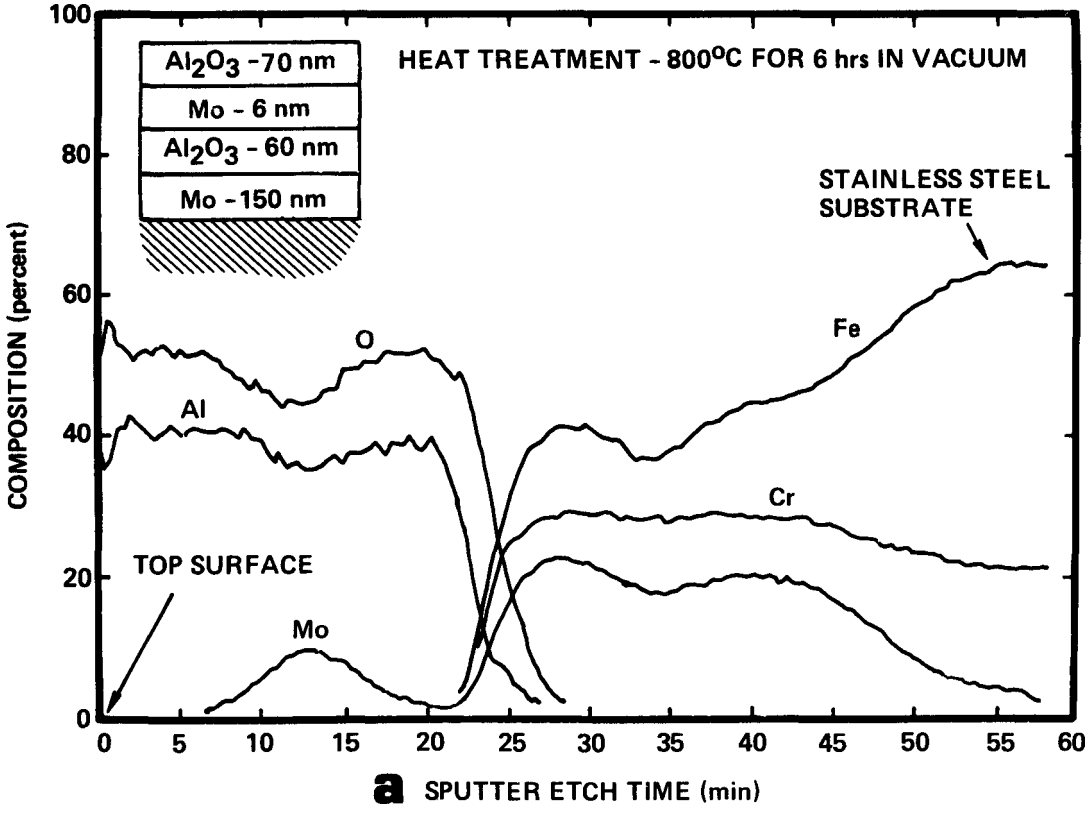

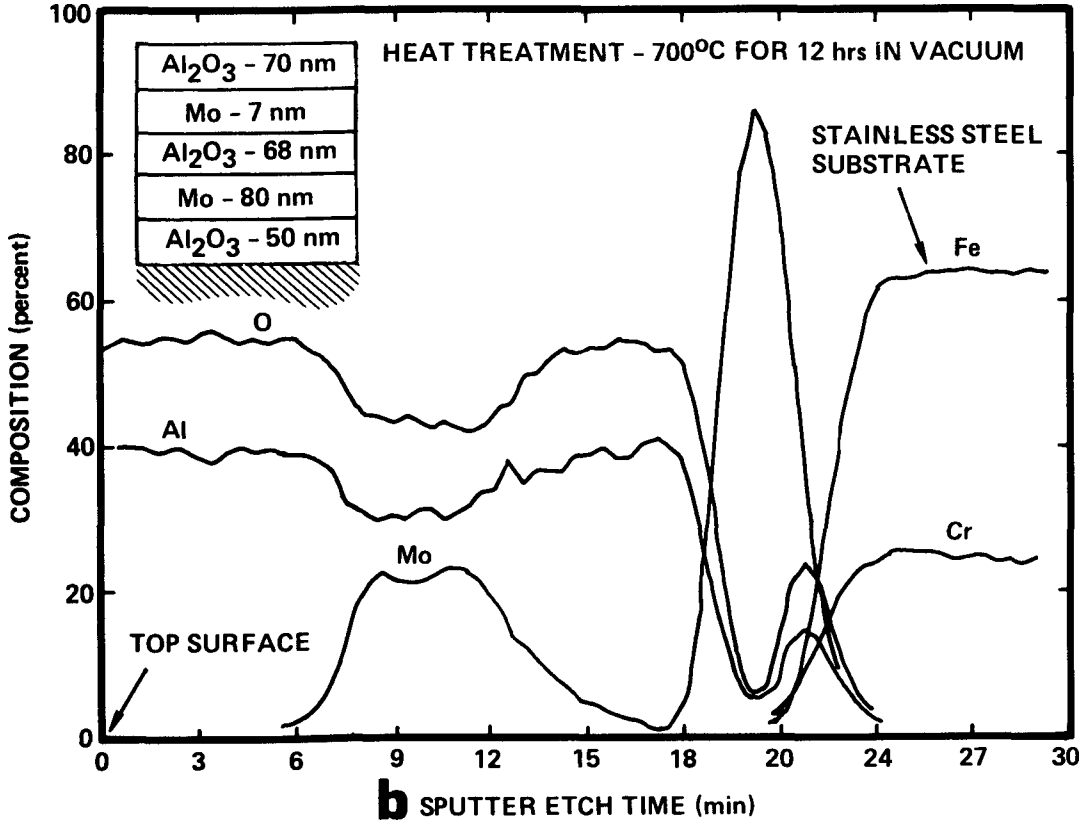

FIG. 16. Auger depth profile composition analyses of Al_2O_3-Mo-Al_2O_3 coatings on Mo coated stainless steel showing effect of heat treatment. The Al_2O_3 layers were formed by direct rf sputtering of alumina.

5. PHASE 3 - CERMET PROOF-OF-CONCEPT

Stainless-steel/CO-cermet coatings of the type described in Section 3.4 were selected for use in the continuous deposition proof-of-concept experiments because of the relatively high rate at which these coatings can be deposited. The coating consists of a thin (40 nm) absorbing layer, formed by sputtering type 304 stainless steel in an Ar-CO gas mixture with a CO injection rate which, for the discharge current of interest, permits the cathode to operate just short of the point of surface poisoning. This layer is overcoated with a dielectric antireflecting layer about 80 nm thick composed of the material that is formed by sputtering stainless steel in pure CO. The coatings yield a solar absorptance of about 0.93 as approximated using an International Technology Alpha Meter, and about 0.89 as determined at the Lockheed Palo Alto Research Laboratory. The emittance is about 0.08 ($20^{o}C$). (See Section 3.4 and Fig. 4).

The experiments were conducted using the apparatus shown in Fig. 17 with a single sputtering source. Thus the strip was moved by the cathode in two passes; i.e., a first pass to deposit the metallic absorbing layer and a second pass to deposit the dielectric layer. The pay-off and take-up reels were 7.6 cm in diameter and accommodated 30 cm wide foil. Aluminum foil strip 30 cm wide x 0.05 mm (0.002 inches) thick and about 12m (40 ft) long was coated in the tests. Coatings were deposited at strip speeds 0.25 and 0.5 cm/sec (0.5 to 1 ft/min). Slight adjustments were made in the discharge current to account for the increase in strip speed which occurred as the foil accumulated on the take-up reel. Both the discharge current and the CO injection were adjusted to account for the overall effect of changing the strip from 0.25 to 0.5 cm/sec. Typical current densities and deposition rates at 0.5 cm/sec were 11 mA/cm^2 and 0.8 nm/s (480 Å/min) for the metallic base layer, and 33 mA/cm^2 and 1.4 nm/s (1000 Å/min) for the dielectric layer.

A few coatings were also deposited at a strip speed of 2 cm/sec (4 ft/min).

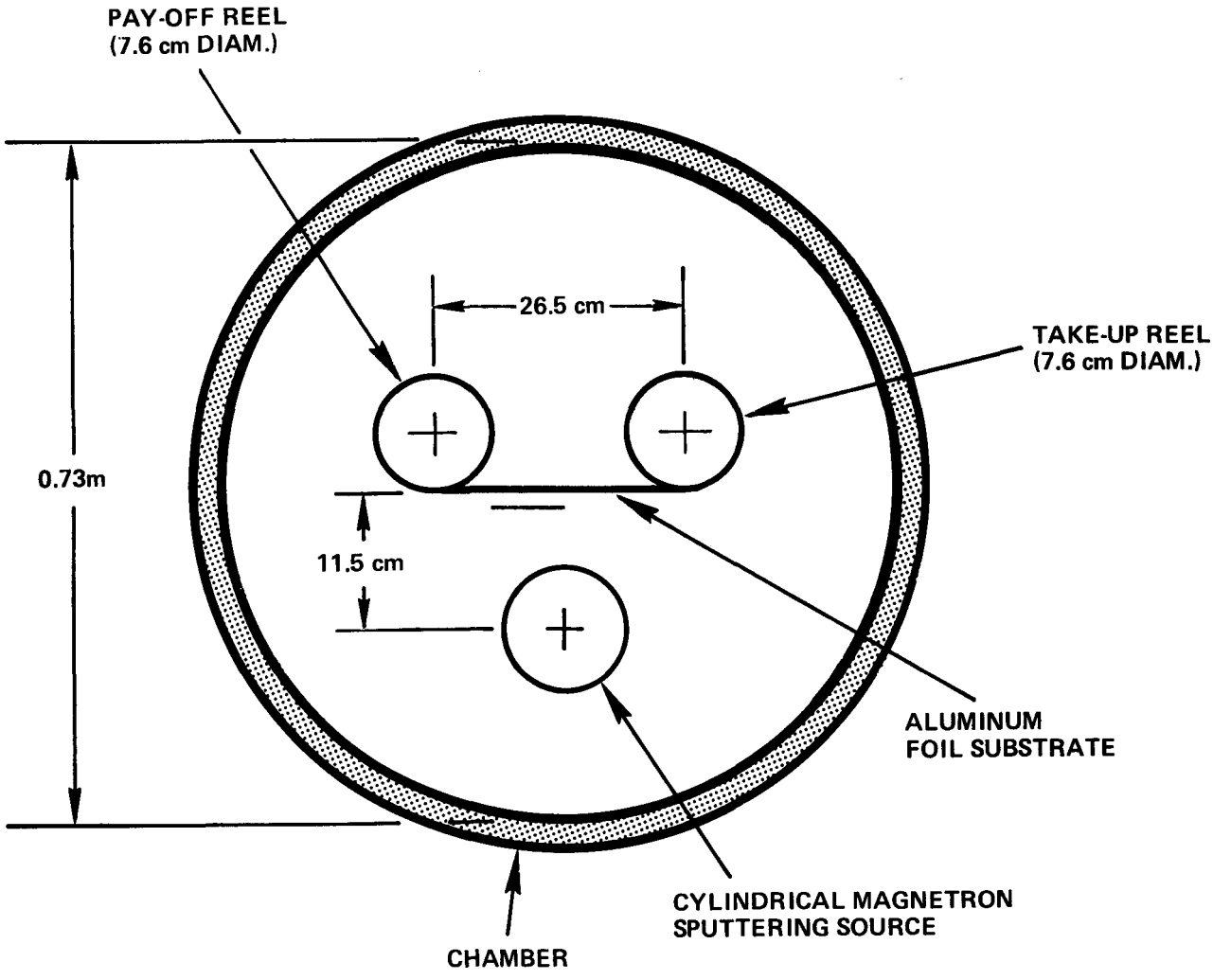

FIG. 17. Schematic illustration of apparatus that was used to continuously deposit selective absorber coatings on aluminum foil strip.

The metal layers were deposited at 2.6 nm/s (1536 Å/min) using a current density of 35 mA/cm^2. The dielectric layers were deposited in multi-passes to simulate the production case where the strip would be passed by a series of cathodes.

Consistent absorptance values of about 0.91 were obtained with the Alpha Meter, indicating that the deposition parameters had been suitably scaled with the strip speed. The emittances were about 0.09. Although these absorptance and emittance values are slightly inferior to those obtained on the static samples (α_H = 0.91 compared to 0.93 and ϵ_H = 0.09 compared to 0.08), the data do indicate that these or similar processes could be scaled to considerably higher strip speeds and optimized to provide higher α_H and ϵ_H values.

6. PHASE 4 - Al_2O_3-Mo-Al_2O_3 PROOF-OF-CONCEPT

The objective in the AMA proof-of-concept experiments was to identify any problems associated with the deposition of Al_2O_3-Mo-Al_2O_3 coatings onto short tubular sections. The tubular substrates were nominally 1.5 cm dia by 10 cm long sections of thin wall type 304 stainless steel tubing. Both the cylindrical-post and cylindrical-hollow magnetron sources were used to coat the tubular sections.

In the cylindrical-post case the tubes were mounted with their axes parallel to the cathode axis, at a distance of 26 cm from the cathode, and rotated at speeds of 1/2 rpm and 7.9 rpm. The substrates were sputter cleaned in Ar (0.2 Pa) at a current density of 1 mA/cm^2 and voltage of about 500V for 5 min prior to coating. The low emittance Mo base layer was about 80 nm thick. The Al_2O_3-Mo(0)-Al_2O_3 coatings had nominal thicknesses of 80 nm/ 10 nm/30 nm (top to substrate) and reactively sputtered Al_2O_3 layers. Deposition shields were used to prohibit coating flux from reaching the tubes at angles greater than about 45^o off the normal.

The hollow cathode apparatus is shown in Fig. 11. A tubular substrate section was mounted on the end of a support rod as shown in the figure. The tubes were vapor degreased in hot trichloroethylene and rinsed in isopropyl alcohol prior to installation in the chamber. No sputter cleaning was used is these experiments, although sputter cleaning would be used in a production coating process. The multilayer Mo-Al_2O_3-Mo-Al_2O_3 coatings were deposited by sequentially passing the substrate into the appropriate deposition sources. The low emittance Mo base layers were about 140 nm thick. The AMA layer thicknesses (top to substrate were about 38 nm/45 nm/ 33 nm.

The optical properties of the coated tubes could not conveniently be measured. However, the general appearance was very similar to that of the flat plates that yielded absorptances greater than 0.90 and emittances less than 0.10. No evidence of poor adhesion was seen on the sputter coated tubes. It is concluded that either hollow cathode or cylindrical-post magnetron sputtering sources could be used to deposit selective surfaces on tubular substrates in large quantities.

7. SUMMARY

Selective absorber coatings deposited by both dc reactive and direct rf sputtering using cylindrical magnetron sources have been investigated. One type of coating consisted essentially of a cermet partially absorbing layer which was overcoated with a non-absorbing antireflective layer. A second type consisted of a multilayer stack of the Al_2O_3-Mo-Al_2O_3 (AMA) type. Substrates were aluminum foil, aluminum coated glass, stainless steel plates and tubes, and stainless steel coated glass.

Three cermet type coatings were examined. In one coating the partially absorbing layer was a 90 nm thick stainless-steel/stainless-steel-oxide cermet formed by reactive sputtering type 304 stainless steel in an Ar-O_2 working gas with pulsed O_2 injection. The antireflecting coating was an

83 nm thick layer of reactive sputtered aluminum oxide. The coatings yielded absorptances of 0.90 and emittances of 0.07 (20°C). The coatings were stable in air at 150°C but underwent slight changes in absorptance in the 200°C to 300°C range.

A second type of cermet coating incorporated a 40 nm absorbing layer formed by sputtering stainless steel in Ar and CO. The antireflecting layer was 90 nm of the dielectric material that is formed by sputtering stainless steel in pure CO. These coatings have yielded absorptances of 0.89 and emittances of 0.08 (20°C). They can be deposited with relatively high rates and were continuously deposited onto 30 cm wide 0.05 mm thick aluminum foil in proof-of-concept experiments. The coatings are stable in air at 150°C but lose absorptance at 200°C.

The third cermet type coating was formed by co-sputtering from Cr and Al_2O_3 (using rf) cylindrical magnetron targets. The coatings were nominally 100 nm thick with a Cr content that varied from about 50 atomic percent to zero over the first 50 nm adjacent to the substrate (aluminum coated glass). The coatings yield absorptances of 0.92 and emittances of 0.07 (20°C) and are expected to possess relatively good thermal stability, although tests were not conducted.

Al_2O_3-Mo-Al_2O_3 coatings with both direct rf sputtered and dc reactive sputtered Al_2O_3 layers have been deposited on both flat plate and tubular substrates. Both cylindrical-post and hollow cathode magnetrons have been used. Coating thicknesses starting at the substrate are typically 80 nm of Mo (low emittance base layer), 300 nm of Al_2O_3 , 10 nm of Mo(0) (Mo sputtered with oxygen injection), and 80 nm of Al_2O_3. Optimum coatings typically exhibit absorptances of 0.94 and emittances of 0.07 (20°C).

The Al_2O_3-Mo-Al_2O_3 coatings appear attractive for a range of solar collector applications. The coatings with reactive sputtered Al_2O_3 layers are stable in air at 300°C. In vacuum they are stable at 400°C but fail at 500°C. The coatings show promise for low cost production in large volume

and should be suitable for medium temperature collectors. AMA coatings with Al_2O_3 layers and diffusion barriers (between the low emittance Mo base layer and the stainless steel substrate) which are formed by direct rf sputtering from alumina targets appear to be stable at 550°C in air and at 700°C in vacuum, although test times were modest (12-15 hrs). These coatings may be adequate for many forms of relatively high temperature collectors. Several aspects of the Al_2O_3-Mo-Al_2O_3 work have been reviewed in Ref. 22.

REFERENCES

1) J. A. Thornton, "Sputter Deposited Selective Absorber Coatings," paper presented at American Electroplaters Soc., Inc., Coatings for Solar Collectors Sym., St. Louis, Missouri (Oct. 1979), published in Plating and Surface Finishing, (Oct. 1980), p. 46.

2) J. A. Thornton and A. S. Penfold, "Cylindrical Magnetron Sputtering," in Thin Film Processes, ed. by J. L. Vossen and W. Kern, Academic Press, New York (1978), p. 75.

3) A. S. Penfold and J. A. Thornton; U. S. Patent 3,884,793 (1975), U. S. Patent 3,995,187 (1976), U. S. Patent 4,030,996 (1977), U. S. Patent 4,031,424 (1977), U. S. Patent 4,041,353 (1977), U. S. Patent 4,111,782 (1978), U. S. Patent 4,116,793 (1978), U. S. Patent 4,116,794 (1978), U. S. Patent 4,132,612 (1979), U. S. Patent 4,132,613 (1979); A. S. Penfold, U. S. Patent 3,919,678 (1975); and J. A. Thornton, U. S. Patent 4,126,530 (1978).

4) J. A. Thornton, "Development of Selective Surfaces," Semi-Annual Technical Progress Report, Sept. 11, 1978 to April 30, 1979, U.S. Department of Energy, contract DE-AC04-78CS35306, Telic Corporation, Santa Monica, CA (June 1979). Available from U.S. DOE-TIA, P.O. Box 62, Oak Ridge, TN 37830.

5) I. T. Ritchie and B. Window, "Applications of Thin Graded-Index Films to Solar Absorbers," Applied Optics, Vol. 16, p. 1438 (1977).

6) G. Hass, H. H. Schroeder and A. F. Turner, "Mirror Coatings for Low Visible and High Infrared Reflectances," J. Opt. Soc. Am., Vol. 46, p. 31 (1956).

7) R. R. Sowel and D. M. Mattox, "Optical Properties and Composition of Electroplated Black Chrome," Plating and Surface Finishing, Vol. 65, p. 50 (Jan. 1978).

8) A. Ignatiev, P. O'Neill and G. Zajac, "The Relationship of Microstructure Optical Properties Relationship in Solar Absorbers: Black Chrome," Solar Energy Materials, Vol. 1, p. 69 (1979).

9) C. M. Lampert and J. Washburn, "Microstructure of a Black Chrome Solar Selective Absorber," Solar Energy Materials, Vol. 1, p. 81 (1979).

10) L. N. Hadley, "Transmittance and Reflectance vs Thickness/Wavelength for Thin Films," available from Colorado State University, Fort Collins, CO.

11) I. T. Ritchie, S. K. Sharma, J. Valignat and J. Spitz, "Thermal Degradation of Chromium Black Solar Selective Absorbers," Solar Energy Materials, Vol. 2, p. 167 (1980).

12) G. Zajac and A. Ignatiev, "High Temperature Optical and Structural Degradation of Black Chrome Coatings," Solar Energy Materials, Vol. 2, p. 239 (1980).

13) R. N. Schmidt, K. C. Park, R. H. Torborg and J. E. Janssen, "High Temperature Solar Absorber Coatings, Part I," Report AD426324 (Nov. 1963). Available from Defense Documentation Center, Alexandria, Virginia.

14) R. N. Schmidt, K. C. Park and J. E. Janssen, "High Temperature Solar Absorber Coatings, Part II," Report AD 455068 (Sept. 1964). Available from Defense Documentation Center, Alexandria, Virginia.

15) R. E. Peterson and J. W. Ramsey, "Thin Film Coatings in Solar-Thermal Power Systems," J. Vac. Sci. Technol., Vol., 12, p. 174 (1975).

16) R. H. Hahn and B. O. Seraphin, "Spectrally Selective Surfaces for Photothermal Solar Energy Conversion," in Physics of Thin Films, ed. by G. Hass and M. H. Francombe, Academic Press, New York (1978).

17) A. B. Meinel, D. B. McKenney and W. T. Beauchamp, "Air-Stable Selective Surfaces for Solar Energy Collectors," Report PB-252 505 (Oct. 1975). Available from National Technical Information Service, U. S. Dept. of Commerce, Springfield, Virginia 22161.

18) L. Chatterjee and K. Prasad, Science and Culture, Vol. 10, p. 559 (1945).

19) R. J. Pressley, Handbook of Lasers with Selected Data on Optical Technology, Chemical Rubber Co., Cleveland, OH (1971) p. 372.

20) R. E. Peterson and J. W. Ramsey, "Solar Absorber Coating Study," Report AD 760577 (May 1973). Available from Defense Documentation Center, Alexandria, Virginia.

21) J. A. Thornton, "Substrate Heating in Cylindrical Magnetron Sputtering Sources," Thin Solid Films, Vol. 54, p. 23 (1978).

22) J. A. Thornton, A. S. Penfold, and J. L. Lamb, "Sputter Deposited Al_2O_3-Mo-Al_2O_3 Selective Absorber Coatings," Thin Solid Films, Vol. 72, p. 101 (1980).

☆U.S. GOVERNMENT PRINTING OFFICE: 1980-740-145/754